Is there enough zooplankton to feed forage fish populations off Peru? An acoustic (positive) answer

Article *in* Progress In Oceanography · December 2011

Impact Factor: 3.03 · DOI: 10.1016/j.pocean.2011.03.001

7 authors, including:

Michael Ballón
Instituto del Mar del Perú
13 PUBLICATIONS **211** CITATIONS
SEE PROFILE

Arnaud Bertrand
Institute of Research for Development
94 PUBLICATIONS **1,884** CITATIONS
SEE PROFILE

Anne Lebourges-Dhaussy
Institute of Research for Development
36 PUBLICATIONS **299** CITATIONS
SEE PROFILE

Patricia Ayón
Instituto del Mar del Perú
33 PUBLICATIONS **459** CITATIONS
SEE PROFILE

Progress in Oceanography 91 (2011) 360–381

Contents lists available at ScienceDirect

Progress in Oceanography

journal homepage: www.elsevier.com/locate/pocean

Is there enough zooplankton to feed forage fish populations off Peru? An acoustic (positive) answer

Michael Ballón [a,b,*], Arnaud Bertrand [a,b], Anne Lebourges-Dhaussy [c], Mariano Gutiérrez [d], Patricia Ayón [a], Daniel Grados [a,b], François Gerlotto [b]

[a] Instituto del Mar del Perú, Esquina Gamarra y Gral. Valle s/n, Apartado 22, Callao, Lima, Peru
[b] Institut de Recherche pour le Développement (IRD), UMR212 EME IFREMER/IRD/UM2, Centre de Recherche Halieutique Méditerranéenne et Tropicale, Avenue Jean Monnet, BP 171, 34203 Sète Cedex, France
[c] IRD, UMR 195 LEMAR, 29280 Plouzané, France
[d] TASA, Av. Néstor Gambeta, Km 14.1, Ventanilla, Callao, Peru

ARTICLE INFO

Article history:
Received 21 July 2010
Received in revised form 11 March 2011
Accepted 14 March 2011
Available online 13 April 2011

ABSTRACT

The Northern Humboldt Current system (NHCS) produces more fish per unit area than any other region in the world. Although the system produces enough macrozooplankton to sustain its high production of forage fish, the paucity of information on macrozooplankton hampers research into the system. In this study, we estimated the biomass of the epipelagic crustacean macrozooplankton from the NHCS during both austral summer and spring 2005. To do this, we developed a bi-frequency acoustic method and extracted high-resolution information on the biomass and the patterns of distribution of crustacean macrozooplankton, fish and other marine compartments. We found that, although macrozooplankton comprises a number of distinct organisms, the euphausiids were the zooplankton group that better fitted the patterns from independent net sampling zooplankton data. Also, the similarities between the nocturnal patterns of size and biomass macrozooplankton distribution from this study and the known patterns of euphausiids, in particular *Euphausia mucronata*, suggest that euphausiids were the main constituent of the estimated nocturnal acoustic macrozooplankton biomass even if other organisms such as large copepods may have contributed considerably to the macrozooplankton biomass. The total macrozooplankton biomass was estimated to about 105 g m^{-2}, i.e., two to five times more than previous estimates. This direct biomass estimation of macrozooplankton is in agreement with the new findings in trophic ecology indicating that forage fish consume mainly macrozooplankton. This high biomass also supports the current hypotheses explaining the NHCS high fish production. Using the method, we are able to revisit present-day and historical acoustic databases and extract high-resolution data on macrozooplankton, a key ecological compartment of the ecosystem. Since zooplankton is the link between the physically driven primary producers and the biologically driven tertiary consumers, this information is essential to achieve a mechanistic understanding of the system, from physics to top predators.

1. Introduction

The northern Humboldt Current system (NHCS) off Peru produces more fish per unit area than any other region of the world ocean. It represents less than 0.1% of the world ocean surface but presently sustains about 10% of the world fish catch (Chavez et al., 2008). Compared with other eastern boundary upwelling systems (EBUS), the higher fish productivity of the NHCS cannot be explained by a corresponding higher primary productivity (Chavez et al., 2008). Since the seminal work of Ryther (1969), Peruvian anchovy (*Engraulis ringens*) was considered to feed directly on phytoplankton, which was not the case for other anchovy species from other EBUS. This short and efficient food chain (Ryther, 1969; Walsh, 1981) was suggested as the reason why the NHCS could sustain such large fish populations. This 'short food chain' hypothesis, however, has recently been discredited by Espinoza and Bertrand (2008) and Espinoza et al. (2009). They showed not only that anchovy and sardine (*Sardinops sagax*) get most of their energy from zooplankton as in other EBUS, but also that macrozooplankton, in particular euphausiids and large copepods, is by far their most important dietary component (in terms of carbon, calorific value). Peruvian anchovy and sardine therefore have a much higher trophic level than previously assumed. Since these species, anchovy in particular, attain very high biomasses, a major change in their diet should arguably affect all other components of the system and thus the carbon flow in conceptual and

* Corresponding author at: Instituto del Mar del Perú, Esquina Gamarra y Gral. Valle s/n, Apartado 22, Callao, Lima, Peru.
E-mail address: michballon@gmail.com (M. Ballón).

0079-6611/$ - see front matter © 2011 Elsevier Ltd. All rights reserved.
doi:10.1016/j.pocean.2011.03.001

trophic models of the NHCS must be re-evaluated. For that purpose, there is a need for quantitative information on the patterns of distribution and abundance of macrozooplankton. This information is required to validate biogeochemical models, adjust trophic models and, more generally, to understand how the ecosystem functions. Unfortunately, the lack of accurate zooplankton data limits our understanding of the system.

In most cases, zooplankton abundance and distribution are assessed by net sampling, which provides data discrete in space and time. Additionally, zooplankton, particularly macrozooplankton, is known to avoid nets (Fleminger and Clutter, 1965; Brinton, 1967; Debby et al., 2004; Lawson et al., 2008) because of both visual and mechanical disturbances (Fleminger and Clutter, 1965); this avoidance being higher when using smaller nets. This avoidance would result in a systematic underestimation of macrozooplankton biomass if the sampling bias is ignored.

Nevertheless, information on zooplankton is available from routine acoustic surveys of finfish species performed by the majority of laboratories all over the world. Because of its non-invasive nature, acoustics can sample organisms that would otherwise be missed by net sampling. Indeed, acoustics allows a simultaneous collection of qualitative and quantitative data on various communities of an ecosystem, from zooplankton to large predators. However, in most cases, acoustic information on zooplankton is considered as noise and is usually eliminated from the data together with that of other non-target species (Bertrand et al., 2003).

Macrozooplankton, like any acoustic scattering group, can be discriminated from other organisms (e.g. fish) using its acoustic properties and its theoretical frequency dependence (Kloser et al., 2002; Logerwell and Wilson, 2004; Mosteiro et al., 2004; Simmonds and MacLennan, 2005). Although the ability to discriminate among scatters groups improves as the number and range of frequencies increase (Napp et al., 1993), to accurately identified the organism, the range of frequencies must extend from the Rayleigh zone (backscattering efficiency increases over the frequencies) to the geometric zone (backscattering efficiency is assumed to remain quite constant) (Holliday and Pieper, 1995). Otherwise, an increase in the number of frequencies does not necessarily translate into higher accuracy (Horne and Jech, 1999).

In marine research institutes, most of present-day and historical acoustic data is recorded at only two frequencies, 38 and 120 kHz. It is the case of the historical acoustic records available in Peru, where the Instituto del Mar del Peru (IMARPE) has routinely used these two frequencies to assess pelagic fish populations. The difference of mean volume backscattering strength between two frequencies (ΔMVBS) is commonly used to determine characteristics of biological backscattering (see Murase et al., 2009). Unfortunately, the power of discrimination between scatterers is limited when applying ΔMVBS only. A recently developed methodology (Lebourges-Dhaussy and Fernandes, unpublished data), based on the sum of backscattering strength (+MVBS) from two or more frequencies enhances the contrast between fish and zooplankton and thus improves their discrimination.

Here, we combined both the ΔMVBS and the +MVBS for discriminating and quantifying the abundance of crustacean macrozooplankton. We applied this method to two routine acoustic surveys performed along the Peruvian coast and showed that: (i) the method is efficient in discriminating between acoustic echoes, (ii) it allows us to provide high-resolution day/night maps of macrozooplankton distribution, (iii) the estimation of macrozooplankton biomass enable us to answer a key question about the system functioning: Is there enough zooplankton to feed the anchovy population off Peru?

2. Materials and methods

2.1. Acoustic data

Acoustic data were collected using hull-mounted Simrad EK500 and EK60 (Kongsberg Simrad AS) split-beam scientific echo-sounders at 38 and 120 kHz during four acoustic surveys performed off Peru on board the IMARPE R/V 'Olaya' (41 m long) (Table 1). Two of these surveys ('Cardumenes 2004' and 'Filamentos 2008') consisted in multidisciplinary specific surveys; while the others ('Pelagic050203' and 'Pelagic051112') were routine acoustic surveys performed by IMARPE for biomass estimation (see Simmonds et al., 2009). Survey tracks consisted of parallel cross-shore transects with a target vessel speed of 10 knots except during the survey 'Cardumenes 2004' where the ship steamed at 8 knots around two, 2-nautical-mile-wide square boxes (see Bertrand et al., 2008).

Echosounder calibration was performed according to Foote et al. (1987). The water column was sampled down to depths of 250 m and 500 m for the 120 kHz and 38 kHz channels, respectively. Due to the presence of noise in the echograms at 120 kHz, only the first 150 m were considered, except in the case of the 'Filamentos 2008' survey, where the employed echo-sounder (EK60) was more efficient. Only day and night periods were considered; data from twilights (sunrise and sunset times plus/minus 10 min) were removed prior to analyses. Also, we only considered data recorded south of 6°S to focus on the NHCS and not on the tropical ecosystem that extends from Northern Peru. Selection, classification and analysis of the acoustic data were conducted with Echoview (SonarData Pty. Ltd., Hobart, Tasmania, Australia) and Matlab (MathWorks™, Natick, Massachusetts, USA) software.

2.2. Net sampling

During routine acoustic surveys ('Pelagic050203' and 'Pelagic051112') zooplankton was collected with Hensen nets of 0.33 m^{-2} mouth area and 300 μm mesh, by vertical hauls between 50 and 0 m (see Ayón et al. (2004) for more information).

Table 1
Acoustic surveys: spatiotemporal extension, acoustic systems and ancillary data.

Survey	Cardumen 2004	Pelagic Summer 2005	Pelagic Spring 2005	Filamentos 2008
Initial	17-11-2004	20-02-2005	25-11-2005	05-02-2008
End	24-11-2004	04-04-2005	24-12-2005	20-02-2008
Latitudinal range	12°34′S–13°40′S	3°29′S–18°03′S	05°11′S–13°28′S	06°30′S–08°02′S
Sampled hours	112	600	840	264
Echosounder system	Simrad EK500 split-beam	Simrad EK500 split-beam	Simrad EK500 split-beam	Simrad EK 60 split-beam
Frequencies	38 and 120 kHz	38 and 120 kHz	38 and 120 kHz	38, 120 and 200 kHz
Plankton multinet sampling	17 profiles			21 profiles
Plankton Hensen sampling		138	96	
Pelagic trawls with simultaneous acoustic records	10 trawls with anchovy and 9 with munida			

During the specific surveys, zooplankton was collected using a vertically profiling plankton net (multinet) with a 300 μm mesh size and 0.25 m^{-2} mouth area in the depth strata 0–10 m, 10–25 m, 25–50 m, 50–75 m, and 75–100 m during the 'Cardumenes 2004' survey and in the depth strata 0–10 m 10–20 m, 20–30 m, 30–50 m, 50–75 m 75–100 m, 100–200 m and 200–300 m during the 'Filamentos 2008' survey.

Zooplankton settled volume (mL) was determined immediately after collection using the displacement method (Kramer et al., 1972). Samples were fixed in 2% formaldehyde buffered with borax, then examined in a laboratory using a stereoscopic microscope to identify and count zooplankton items.

Fish and the squat lobster (*Pleuroncodes mondon*), a pelagic crustacean highly abundant since the mid-1990s (see Gutiérrez et al., 2008), were collected by pelagic trawl 'Engel 124/1800' (12 mm codend mesh). For each trawl, a subsample of the catch was collected and individuals were identified and sized.

2.3. Acoustic data analysis

To compare the echograms, we synchronised the ping number and position between echograms using the matching ping number algorithm from Echoview. We excluded the noise from the surface (5 m depth from the transducer) and the bottom echo. We cleaned the echograms by defining and eliminating parts of the echograms in which noise could have affected further analysis. We considered noise as everything apart from the transmitted sound backscattered onto the transducer surface (see Korneliussen, 2000). We also excluded regions below compact and/or large fish schools, whose presence diminish the acoustic signal (see Gerlotto, 1996) in such a way that it becomes too weak to properly sample the layers below the school. To eliminate the noise associated with the acoustic absorption we followed the method proposed by Fernandes et al. (2006) and created a new acoustic field for each frequency using a data generator algorithm from Echoview based on a noise function with the form:

$$20\log(R) + 2\alpha R + offset \quad (1)$$

where R is the range (in m), α is the frequency absorption coefficient (in dB m^{-1}) and the *offset* value (in dB) is the assumed initial noise at the first metre. To generate the noise field we need initial input values of α and the *offset*. These values were determined from the minimum noise values per depth estimated from an echogram section below the bottom (Matlab program developed by P. Fernandes, Marine Lab., Scotland, UK). The noise field generated from Eq. (1) was subtracted from the echogram in the linear domain. Finally, we resampled the bi-frequency echograms in common elementary cells 1 ping long and 0.75 m high.

To enhance the contrast between fish and macrozooplankton backscatter we used a recently developed methodology (Lebourges-Dhaussy and Fernandes, unpublished data) and summed the mean volume backscattering strength between the two frequencies (+$MVBS_{120+38}$). This complements the power discrimination of $\Delta MVBS_{120-38}$, which does not allow for situations that may be encountered at sea (e.g., the presence of pneumatophores that, depending on their size, may display an increasing or decreasing trend between the 38 and 120 kHz frequencies). Also, if the range 38–120 kHz falls within the transition zone, where backscatter efficiency of the organisms is not monotonic and fluctuates over the frequencies (Stanton et al., 1998), ΔMVBS may be positive or negative. So, regardless of the trend of the $\Delta MVBS_{120-38}$, the difference in variability between fish and macrozooplankton was used to enhance the contrast between both types of organisms (Lebourges-Dhaussy and Fernandes, unpublished data). Based on observations, we then empirically chose a threshold value of −135 dB for the sum echogram (+$MVBS_{120+38}$) and used a Boolean mask (true for values above threshold) to extract fish data from other scatters and create "fish" and "no fish" echograms at each frequency. The "no fish" echogram is just a schematic denomination but it does not imply that this category is free from other weak fish scatter (e.g. fish larvae or juveniles). All post-processing processes were applied equally to both frequencies.

In the NHCS, all exploited fish (anchovy, sardine, jack mackerel *Trachurus murphyi* and mackerel *Scomber japonicus*) and most mesopelagic fish are swimbladder-bearing. Therefore, any reference to 'fish' in this study pertains to swimbladder-bearing fish. Swimbladder-bearing fish have slightly higher backscatter at 38 than 120 kHz (Kloser et al., 2002), but some rare cases of positive $\Delta MVBS_{120-38}$ (up to ∼+2 dB) can be observed in the fish data. We thus refined the fish data from the fish echograms by applying a second Boolean mask to keep only the targets for which $\Delta MVBS_{120-38} < +2$ dB.

Zooplanktonic organisms with weakly scattering tissue and acoustic properties similar to the medium are usually named "fluid-like" zooplankton (Stanton et al., 1996). The "fluid-like" group includes euphausiids, copepods, salps, siphonophores (without gas bladders) and other large crustacean macrozooplankton (e.g. squilla larvae, galatheid and other decapod larvae). This group was extracted from the "no fish" echograms by applying a Boolean mask to select the targets with positive $\Delta MVBS_{120-38}$. Targets with negative $\Delta MVBS_{120-38}$ were named "blue-noise". This group enclosed all targets different from fluid-like macrozooplankton and fish (mainly fish larvae, gelatinous and gas-bearing siphonophores).

A preliminary examination of the fluid-like echograms revealed that some targets located inside or at the edge of fish schools were inaccurately selected as fluid-like organisms. To correct this problem we developed a 4-step procedure to extract the remaining fish backscatters from the fluid-like echograms and include them into the fish echograms:

(i) a copy of the fish echograms was smoothed by applying a 3 × 3 convolution matrix where all kernel cells in the convolution matrix were set to 1 (convolution operator from Echoview). This resulted in an "expanded" version of the fish echogram in which the value of a cell was replaced by the mean value resulting from the average with its immediate eight 'neighbour' cells;
(ii) the expanded fish echograms were used to create a Boolean mask, with false values where fish were present;
(iii) we applied this mask to the non-expanded echograms to create new no-fish echograms;
(iv) we applied the Boolean mask again to select the targets with positive $\Delta MVBS_{120-38}$ to create new fluid-like echograms.

Although, the new fluid-like echograms were almost free from fish echoes, some of the fluid-like targets were eliminated too. These gaps were filled in the final fluid-like echogram by combining the new fluid-like echogram and an expanded version of it according to a logical bitmap ("select" operator from Echoview). This bitmap has true values for the cells where the original fluid-like echogram has a correspondence value in the new fluid-like echogram and false otherwise. If there was a true value in the bitmap then the corresponding data value from the new fluid-like echogram was used, otherwise the corresponding data from its expanded version was used. A similar procedure was used to include the fish echoes extracted from the fluid-like echograms into the final fish echograms.

To eliminate potential remaining high noise echoes on the echograms of major scatter groups (fish at 38 kHz, blue-noise at 38 kHz, fluid-like at 38 kHz and 120 kHz) based on visual scrutinizing, we applied the following upper thresholds: −21 dB for fish,

−56 dB for blue-noise and −53 dB for fluid-like (120 kHz). Finally we excluded fish and blue-noise echoes lower than −100 dB from the analysis.

We discriminated the squat lobster *Pleuroncodes mondon* from other fluid-like organisms for several reasons: (i) squat lobsters are larger than any other fluid-like macrozooplankton in the ecosystem and do not play the same ecological role (e.g. adult squat lobsters are not foraged by small pelagic fish), (ii) squat lobsters have stronger backscatter than other fluid-like organisms present, (iii) off Peru, squat lobsters are epipelagic and perform vertical migrations inside the epipelagic layer (Gutiérrez et al., 2008). To extract the squat lobster from other fluid-like scatters we applied the following thresholds on the fluid-like group S_{v120}: $-72\ \text{dB} < S_v < -53\ \text{dB}$. The thresholds limits were determined empirically from echograms where the presence or absence of squat lobster was confirmed from pelagic trawls. The squat lobster has a very characteristic spatial distribution. The resulting squat lobster echogram was validated by both ground-proofed squat lobster records along transects (the squat lobster is routinely assessed by IMARPE) and their position within the epipelagic layer.

2.4. Fluid-like biomass estimation

Although the fluid-like group includes euphausiids, copepods, salps, siphonophores (without gas bladders) and some squat lobster juveniles, we focused on large macrozooplankton; mainly euphausiids, but also large copepods. This was because small fluid-like crustacean zooplankton (e.g. small copepods) cannot be properly detected and quantified using the 38 kHz (Mitson et al., 1996). Salps are not common outside the northern area (further north than 6°S, area not included in this study) (Ayón et al., 2008a), siphonophores without gas inclusion have a very low biomass (Ayón et al., 2008a) and squat lobster juveniles would only be important in near-coastal areas (Fagetti and Campodonico, 1971). On the other hand, euphausiids and large copepods, particularly *Eucalanus* spp., are the most abundant macrozooplankton groups (Ayón et al., 2008a) and the main prey of the most abundant fish species: anchovy, sardine, mackerel, jack mackerel and mesopelagic fish (Konchina, 1981; Espinoza and Bertrand, 2008; Espinoza et al., 2009). According to Murase et al. (2009) large copepods need to occur in high densities to be detected by the 38 kHz frequency. Since euphausiids attain a larger biomass than copepods (Ayón et al., 2008a) and are preferentially foraged (e.g. Espinoza and Bertrand, 2008), we designed the method according to euphausiids acoustic properties to estimate the biomass of macrozooplankton.

While the shape of euphausiids is more cylindrical than spherical, in practice the fluid sphere model based on two frequencies is appropriate when estimating zooplankton biovolumes (Holliday and Pieper, 1995). The imperfect representation of the shape becomes negligible once averaged with many echoes and when the range of orientation of the animals includes broadside incident (Stanton and Chu, 2000).

To estimate the mean size (radius of the sphere), the number of insonified organisms and then the fluid-like biovolume per cell in the echogram, we applied a method based on the S_v difference between frequencies (Greenlaw, 1979).

Determination of the sphere radius (a) using the fluid sphere high-pass model (Johnson, 1977):

$$(ka)^4 = (2/3).[(r^4 - R)/(r^2(R-1))] \quad (2)$$

where $k = 2\pi f_m/c$, a = the radius of the sphere (in m), c = speed of sound (in m s^{-1}), $f_m = (f_{120} \cdot f_{38})^{0.5}$ (in Hz), $r = f_{120}/f_{38}$, and $R = 10^{(Sv(120)-Sv(38))/10}$. The speed of sound was assumed to be: 1509 m s^{-1} corresponding to a mean temperature of 15.5 °C and a salinity of 35 psu.

Then, the determination of the backscattering cross-section σ_{bs} of the sphere can be estimated according to Greenlaw (1979):

$$\sigma_{bs} = [(1 - gh^2)/(3gh^2) + (1-g)/(1+2g)]^2 \cdot a^2 \cdot [2(ka)^4/(2 + 3(ka)^4)], \quad (3)$$

where g is the density contrast between the sphere and the surrounding medium, and h the speed contrast. No estimation of g and h are available for *Euphausia mucronata*, the dominant euphausiids species in the HCS. Consequently, we used the parameters estimated for a similar species, *Euphausia pacifica*, from the California Current system. For that we averaged the results obtained by Greenlaw and Johnson (1982) based on freshly caught *E. pacifica* (g = 1.037, and h = 1.0097).

According to Mitson et al. (1996), the ratio of 120–38 kHz allows safe estimates of length over a *ka* range of 0.4–1.6, which correspond to a S_v difference of 18.5 and 3 dB respectively. When this difference is too small (<2 dB) or too large (>19 dB), the radius of the sphere a tends to be overestimated or underestimated, respectively (figure not shown). For this reason only the differences comprised between 2 and 19 dB were used for the biovolume estimation. Although this could lead to an underestimation of the biovolume, in practice most of the observed S_v differences for fluid-like lay within this range.

The number of individuals per unit volume (N_f, in ind m^{-3}) can be estimated as follows:

$$N_f = 10^{(Sv(f)-TS)/10} \quad (4)$$

where $TS = 10\log_{10}(\sigma_{bs})$.

Fluid-like biovolume was calculated by multiplying the densities of the organism (ind m^{-3}) by the volume (in cm^3) of the sphere of radius a, i.e. the estimated volume of each 'average' individual.

Fish, blue-noise and squat lobster S_v were converted into acoustic nautical area scattering coefficient (NASC), an index of abundance, according to MacLennan et al. (2002):

$$\text{NASC}\ \ (\text{in m}^2\ \text{n mi}^2) = 4\pi(1852)^2 s_v T, \quad (5)$$

where T is the integrated vertical distance of the elementary cells of 0.75 m.

2.5. Vertical extension of the epipelagic community

The NHCS is characterised by the presence of one of the most intense and superficial oxygen minimum zones (OMZ) of the world ocean (Helly and Levin, 2004; Chavez and Messié, 2009; Paulmier and Ruiz-Pino, 2009). Although some species of zooplankton, mesopelagic fish and squids have adapted their metabolism to temporarily (through diel vertical migration) or permanently inhabit OMZs, the vertical extension of the zooplankton epipelagic community (VEEC) is usually limited by the presence of the OMZ (Ayón et al., 2008a; Criales-Hernández et al., 2008; Bertrand et al., 2010), which forms a sharp barrier to most marine species. We defined the VEEC depth (Z_{VEEC}) to be the depth where 98% of the cumulative sum of acoustic echoes from the epipelagic community was reached (Bertrand et al., 2010). Z_{VEEC} was corrected to take into account the transducer position on the R/V hull (3.4 m below the sea surface).

Anchovy, the dominant epipelagic fish in the system, have a much higher target strength (∼−50 dB) than euphausiids (∼−85 dB), but fish generally occupy only a small part of the epipelagic habitat observed in the echogram while macrozooplankton (mainly crustaceans and gelatinous organisms) fills most of the echogram. Therefore, to better reflect the actual distribution of the overall epipelagic community, we considered all echoes but minimized the weight of fish echoes by a factor 10^{-3} when

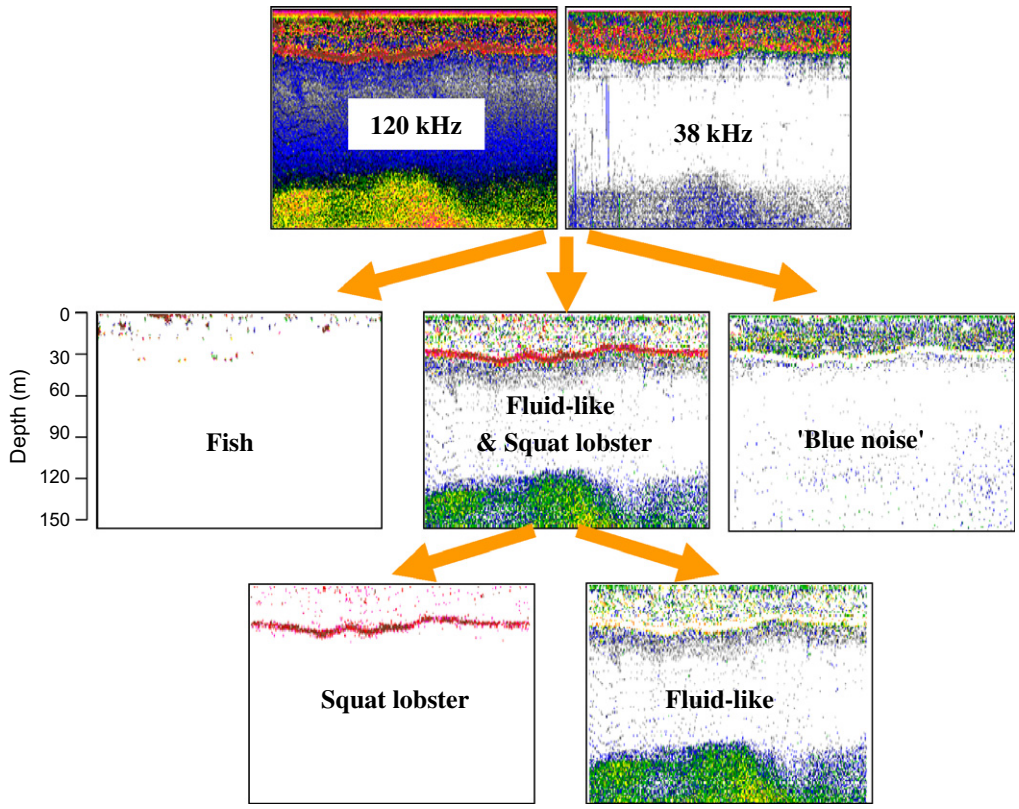

Fig. 1. Example of application of the bi-frequency acoustic algorithm to discriminate the following scatter types: fish, 'blue-noise', fluid-like and munida.

estimating Z_{VEEC}. The mean concentration in dissolved oxygen at Z_{VEEC} was 0.80 mL L^{-1}, independent of the diel period (Bertrand et al., 2010).

In the HCS the main euphausiids and *Eucalanus* species are adapted to hypoxia and inhabit the OMZ during the day (Antezana, 2010; Escribano et al., 2009). During the night, however, they migrated toward the surface and became part of the epipelagic community, affecting its species composition and biomass (Antezana, 2010; Escribano et al., 2009). Therefore, independent estimates of epipelagic macrozooplankton biomass were made for the day and the night-time periods.

To estimate the integrated macrozooplankton biomass (in g m^{-2}) of the epipelagic layer we performed the following steps:

(i) we reduced the echograms (fluid-like, fish and blue-noise) by calculating the median value for every three pings;
(ii) using these "reduced echograms" we estimated Z_{VEEC} according to the procedure described before (see Bertrand et al., 2010) and used it to delimit the epipelagic layer;
(iii) we estimated the mean fluid-like biovolume and size of the macrozooplankton contained within the epipelagic layer. From this step, an elementary acoustic cell is 3 pings long and has a height equal to Z_{VEEC}. Since each elementary acoustic cell of an echogram was assigned to one sole scatter group according to the properties of the dominant echoes composing it, weak scatters would be 'hidden' when strong scatters were present in the same elementary acoustic unit. Thus, if fluid-like was present together with fish, the later would dominate and it would not be possible to detect the presence of fluid-like (Korneliussen and Ona, 2003). To reduce this bias, the mean fluid-like biovolume and size were estimated without including the cells assigned to other scattering groups;
(iv) fluid-like mean density in wet weight (*WW*, in g m^{-3}) was estimated according to functional regression equations between these variables and fluid-like biovolume (Wiebe et al., 1975; Wiebe, 1988):

$$Log(Bv) = 0.139 + 1.003 * Log(WW) \quad (6)$$

where *Bv* is the fluid-like mean biovolume (in cm^3 m^{-3}) in the epipelagic layer;

(i) the integrated macrozooplankton biomass of the epipelagic community per elementary sampling unit was then estimated by multiplying their mean density by ZVEEC.

Day and night data were classified according to the ecological domains (shelf, slope and offshore); then, the total acoustic biomass/size per survey and diel period was estimated as the mean of the biomass/size from the shelf, slope and offshore domains weighted by the area occupied by each domain. A similar procedure was performed to estimate the total macrozooplankton biomass from net sampling per survey and diel period.

To estimate the macrozooplankton biomass within the area of anchovy distribution, we delimited such areas using ground-proofed anchovy records from the 'Pelagic050203' and 'Pelagic051112' surveys and then estimated the macrozooplankton biomass within and outside this area.

2.6. Validation

The validation of the acoustic methodology was performed in three steps. First, we compared the acoustic biomass (NASC) of fish and squat lobster from the 'Cardumen 2004' survey with their respective catches from pelagic trawl net sampling. To ensure comparable catches, the velocity (~2 knots) and duration (20 min) were kept constant when trawling. The acoustic fish and squat

lobster NASC comprised within the 10 central minutes of trawl net sampling were used for this comparison.

Second, we compared the vertical profiles of fluid-like acoustic biovolume with those of zooplankton biovolume from multinet samples at different depth strata during the 'Cardumen 2004' survey. Also, the integrated abundance (10–100 m) of the most important macrozooplankton (adult euphausiids, squat lobster zoea, *Eucalanus inermis* and euphausiid larvae and juveniles) was compared with the integrated acoustic biovolume of fluid-like macrozooplankton. As there were no acoustic records during the net sampling, we used the 25 pings recorded just before the multinet profile took place.

Third, we compared the vertical profiles of fluid-like acoustic biovolume with the abundance of euphausiid adults, juveniles and larvae sampled with the multinet. We used data acquired during the 'Filamentos 2008' survey, where bi-frequency acoustic data are available until 300 m depth. Since in this survey there were simultaneous acoustic records and multinet sampling, the acoustic records obtained within the time of multinet sampling were used to estimate fluid-like biovolume. Here we only used multinet sampling stations at a depth exceeding 300 m (9 out of 21).

We acknowledge the limitation of the vertical net sampling with a small mouth area when properly sampling macrozooplankton, particularly the relatively fast swimmer species such as euphausiids. While oblique tows carried out by net systems with a larger mouth area would have provided a more reliable estimation of macrozooplankton biomass, those net systems have rarely been used in the NHCS. In this system, the only source on which historical acoustic patterns could be compared come from vertical net sampling with a rather small mouth area as previously described. We are assuming however, that these nets can still catch enough macrozooplankton to allow extracting the main characteristics of their vertical and horizontal distribution patterns.

2.7. Patterns of distribution of fluid-like biomass

For each diel period, broad patterns of macrozooplankton distribution according to the ecological domain, distance to the shelf break (every 10 km interval) and latitude were represented using box plots. Box plot is a graphical method for displaying the median, the upper and lower quartiles, and the minimum and maximum data values. To dismiss a possible effect of an overrepresentation of any ecological domain in a particular latitudinal degree due to the sampling strategy, the box plots per latitudinal degree were also constructed for each ecological domain and compared to the one obtained from the pooled data.

Since the box plots showed that the macrozooplankton biomass data were positively skewed, these data were normalized by applying cubic root transformation before applying any statistical test. We used an ANOVA to test the diel effect within each ecological domain independently. We also applied an ANOVA with further post hoc Turkey test to assess if macrozooplankton biomass significantly differed between domains.

We constructed interpolated day and night maps of macrozooplankton biomass by kriging for the spring and summer surveys of 2005. Because the spatial distribution of macrozooplankton biomass was anisotropic, with higher autocorrelation in the alongshore direction than in the across-shore direction, we fitted a directional variogram on the data. These maps were then compared with the corresponding plots of zooplankton biomass from net samplings.

3. Results

3.1. Validation

The first step of the validation of the bi-frequency algorithm (Fig. 1), the comparison of acoustic NASC and net sampling captures of fish and squat lobster, showed that fish and squat lobster from these two sources were significantly positively correlated (fish: $p = 0.006$, $r^2 = 0.62$; squat lobster: $p = 0.008$, $r^2 = 0.56$).

Macrozooplankton mean biovolume from the acoustic method was 1 order of magnitude higher than the biovolume from net samples. There was however an agreement between the vertical profiles of fluid-like biovolume from acoustic and net sampling during both day and night (Fig. 2).

The second step of the validation consisted in the comparison of the patterns of integrated abundance (vertical range: 10–100 m) of adult euphausiids (Fig. 3a), squat lobster zoea (Fig. 3b), *Eucalanus inermis* (Fig. 3c) and euphausiid larvae and juvenile (Fig. 3d) with the integrated fluid-like acoustic biovolume. The results showed that adult euphausiids was the group with the most similar pattern to the pattern of the integrated fluid-like acoustic biovolume. It is worth mentioning that biovolume not only depends on the organism's abundance but also on its size and shape. However, when working with a relatively homogenous group (e.g., zoea of squat lobster, adult euphausiids) the effects of different sizes or shapes are assumed to be minimal when compared with the effect of organism abundance.

The importance of euphausiids as the main responsible organism for the observed acoustic pattern was also confirmed by the comparison of fluid-like acoustic biovolume and multinet abundance estimates of euphausiids per depth stratum during

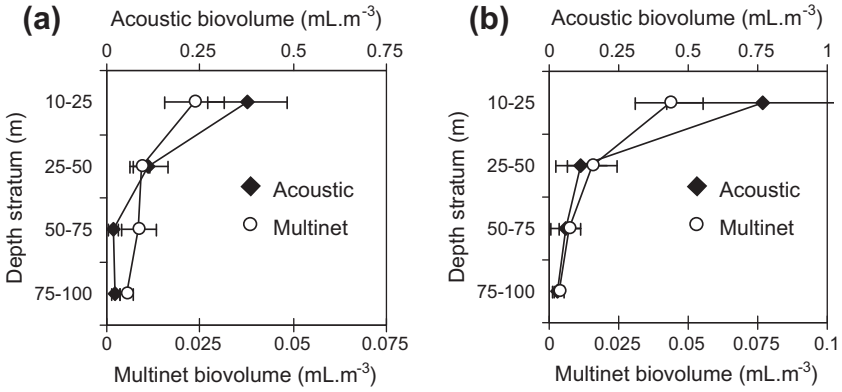

Fig. 2. Day (a) and night (b) mean macrozooplankton biovolume (mL m^{-3}) and confidence interval (horizontal segments) per depth stratum estimated by multinet (open circle) and acoustic (plus symbol) (data from 'Cardumen 2004' survey).

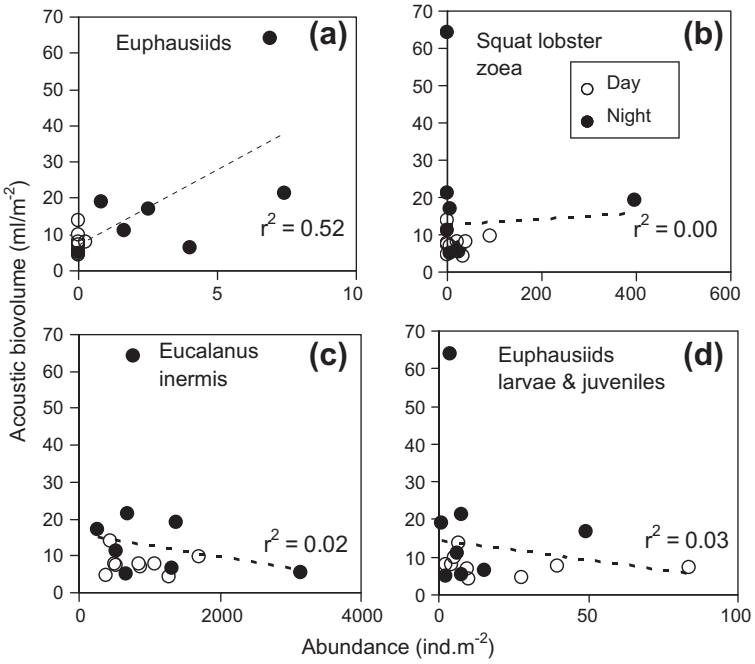

Fig. 3. Scatter plot of acoustic biovolume (in mL m^{-2}) and multinet abundance (in ind m^{-2}) of adult euphausiids (a), munida zoea (b), *Eucalanus inermis* (c) and euphausiids larvae and juveniles (d) integrated from 10 to 100 m (data from 'Cardumen 2004' survey).

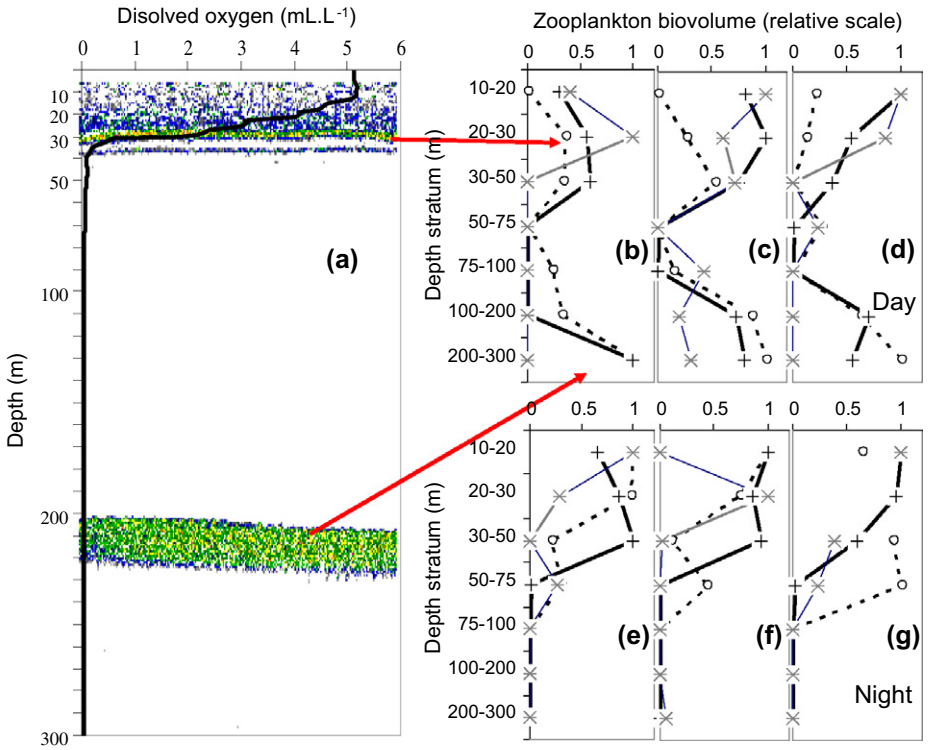

Fig. 4. Comparison of fluid-like acoustic biovolume and multinet abundance estimations of euphausiids per depth strata during the Survey 'Filamentos 2008'. Each profile (b, c, d, e and f) corresponds to one multinet sampling station. (a) fluid-like echogram with an overlaid dissolved oxygen profile corresponding to the vertical profile showed in (b). Day-time (b–d) and night-time (e–h) vertical profiles of abundance of adults euphausiids (plus symbol) and euphausiids larvae–juveniles (asterisks) from multinet and fluid-like macrozooplankton biovolume from acoustic (solid diamond symbol). Abundance/biovolume were standardized by dividing the abundance/biovolume of a stratum by the maximum abundance/biovolume of the profile.

the survey 'Filamentos 2008' (third step). Multinet samples showed that euphausiid adults, juveniles and larvae were abundant in the epipelagic layer during the day (Fig. 4b–d). An intermediate zone, almost free of euphausiids, was located between the upper and deeper euphausiid layers. The deeper layer, which was observed between 200 and 300 m (i.e. in the core of the OMZ), consisted of adult euphausiids only. During the night (Fig. 4e–g), euphausiids were distributed only in the epipelagic layer, whatever

their ontogenic stage. Acoustic vertical profiles of fluid-like biovolume presented very similar patterns of vertical distribution. Note the two diurnal dense scattering layers, one epipelagic, the other bathypelagic, observed in the acoustic echogram (Fig. 4a) corresponding to the two picks of euphausiid catches (Fig. 4b).

3.2. Diel variation on macrozooplankton biomass and size

Total nocturnal macrozooplankton epipelagic biomass from acoustic data was estimated to be 105.7 and 103.8 g m^{-2} during 2005 austral summer and spring, respectively (Fig. 5). These night-time estimates were about four times higher than diurnal biomasses: 26.15 and 21.9 g m^{-2} during 2005 austral summer and spring, respectively.

Macrozooplankton estimated sizes were slightly different according to diel cycle, but very similar between surveys (Fig. 6). In both surveys, the estimated macrozooplankton size was about 5% larger during the night than during the day. Macrozooplankton size must be understood as the radius of the fluid sphere which is assumed to have the same volume as a 'mean macrozooplankton organism'; it is the Equivalent Spherical Radius or ESR. Nocturnal zooplankton biomass from net sampling was estimated to be 21.2 and 22.1 g m^{-2} during 2005 austral summer and spring, respectively. The corresponding diurnal zooplankton biomass was estimated to be 12.9 and 13.8 g m^{-2} during summer and spring, respectively.

3.3. Macrozooplankton biomass and size by ecological domains

Macrozooplankton epipelagic biomass (transformed by cubic root) varied significantly with the ecological domain (Fig. 7) during both day (ANOVA: $F_{[2,\ 115020]} = 10758.1$, $p = 0.0001$ for summer survey and $F_{[2,\ 132416]} = 22699.5$, $p = 0.0000$ for spring survey) and night (ANOVA: $F_{[2,\ 91995]} = 25249.8$, $p = 0.0001$ for summer survey and $F_{[2,\ 96455]} = 18912.5$, $p = 0.0001$ for spring survey). In all cases post hoc Turkey tests were significant ($p < 0.05$). Macrozooplankton biomass increased across the continental shelf, slope and toward the offshore area whatever the survey or the diel period considered (except during the day in February–March 2005 when the biomass was slightly lower in the shelf break compared with

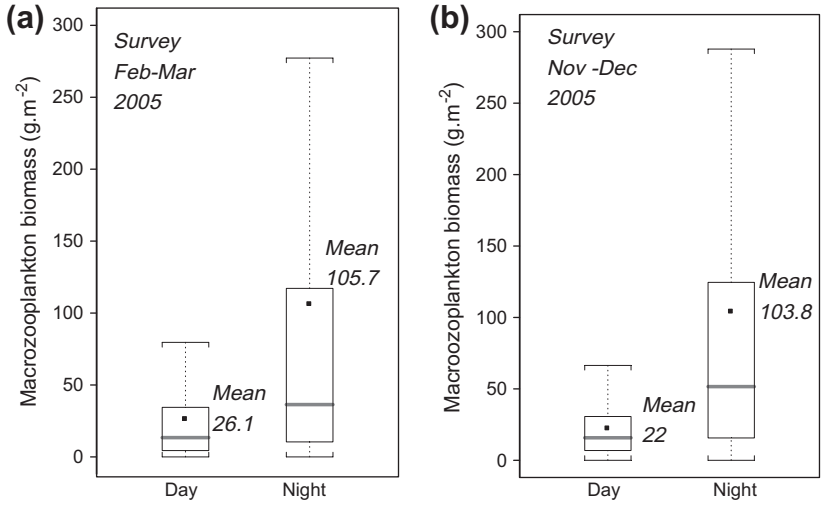

Fig. 5. Box plot of day and night epipelagic macrozooplankton biomass (g m^{-2}) during austral summer (a) and spring (b) pelagic surveys 2005. The size of the box is determined by the upper and lower quartiles, median is indicated as a horizontal line inside the box. Weighted mean is represented as a black solid square point. The whiskers indicate the minimum and maximum values without considering outliers.

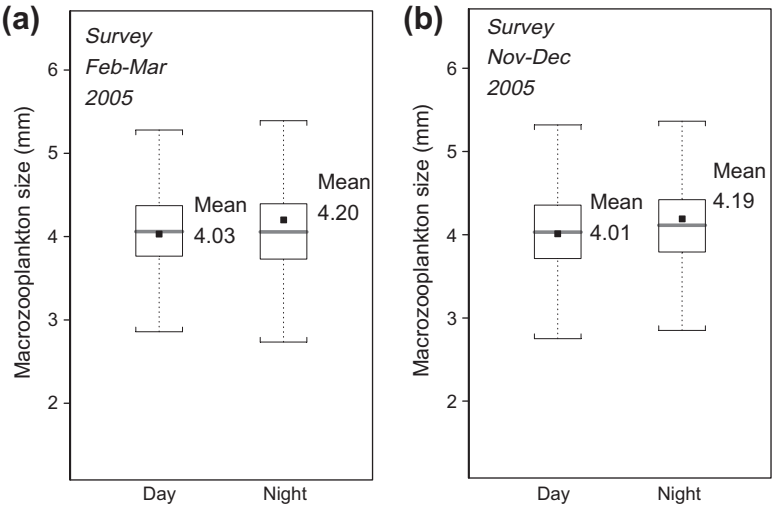

Fig. 6. Box plot of day and night epipelagic macrozooplankton ESR (mm) during Austral summer (a) and spring (b) pelagic surveys 2005 (for details on box plot see the caption of Fig. 5).

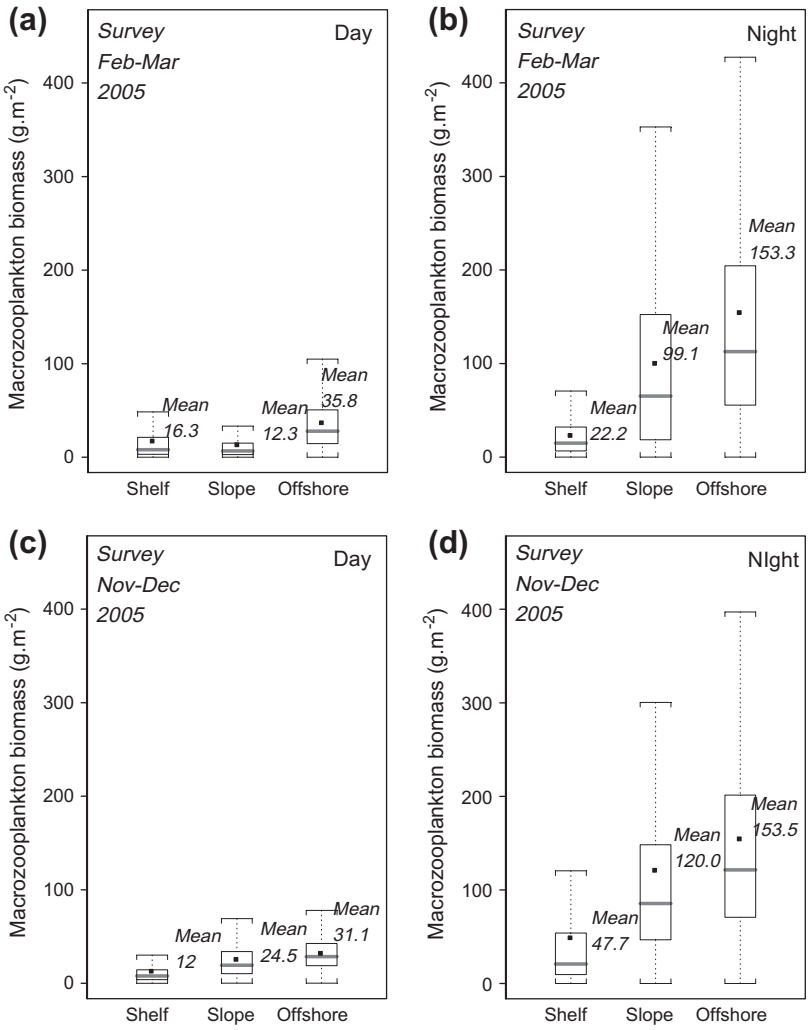

Fig. 7. Day and night box plots of epipelagic macrozooplankton biomass (in g m^{-2}) according to the shelf, slope and offshore ecological domain for both Austral summer (a and b) and spring (c and d) 2005 (for details on box plot see the caption of Fig. 5).

the shelf). In the area of spatial overlap with anchovy distribution, nocturnal macrozooplankton biomass was estimated to be 55 and 52 g m^{-2} during 2005 austral summer and spring, respectively. In the offshore non-overlapping area, macrozooplankton biomass was estimated to be 161 and 135 g m^{-2} during 2005 austral summer and spring, respectively.

Macrozooplankton sizes exhibited less variation according to the ecological domain during the day than during the night (Fig. 8). Whatever the survey or the diel period, macrozooplankton were significantly larger offshore than in the shelf (ANOVA and Turkey post hoc results not shown). The size pattern of macrozooplankton distributed in the slope was variable. Compared with the shelf, the size of macrozooplankton distributed over the slope was significantly larger in spring 2005 during the night, significantly smaller in summer 2005 during the night, and not significantly different in the other cases. Finally, in each survey, macrozooplankton size was significantly larger during the night than during the day and this pattern was particularly pronounced offshore.

3.4. Across-shore distribution of macrozooplankton biomass, density and size

Previous results showed that macrozooplankton biomass increased from the coast toward offshore waters. A more detailed description of the across-shore distribution of macrozooplankton biomass (Fig. 9) illustrates the importance of the shelf break as a cut-off point with higher biomasses offshore, in particular during the night. Offshore, macrozooplankton biomass and density (the plots for density are not shown since they are very similar to the one for biomass) increase with the distance to the shelf break but with a different pattern according to the survey. In the summer survey, the offshore macrozooplankton biomass and density increased with the distance to the shelf break (Fig. 9b). In contrast, during the spring survey, macrozooplankton biomass and density exhibited a bell-shaped pattern with the highest values around 50 km offshore from the shelf break and a decreasing trend thereafter (Fig. 9d).

The broad patterns in across-shore macrozooplankton size distribution presented in Fig. 8 are described in more detail in Fig. 10. This figure shows the high variability in macrozooplankton size at any point, probably illustrating the diversity in size of the epipelagic macrozooplankton community. The across-shore trend of increasing macrozooplankton size was clear during the night but not obvious during the day. During the austral summer survey and at night the largest sizes were observed in the farthest offshore area. During the austral spring survey, the nighttime size estimates increased until around 50 km offshore and then stabilized. Large macrozooplankton also occurred in the closest coastal areas whatever the survey and the diel period (Fig. 10).

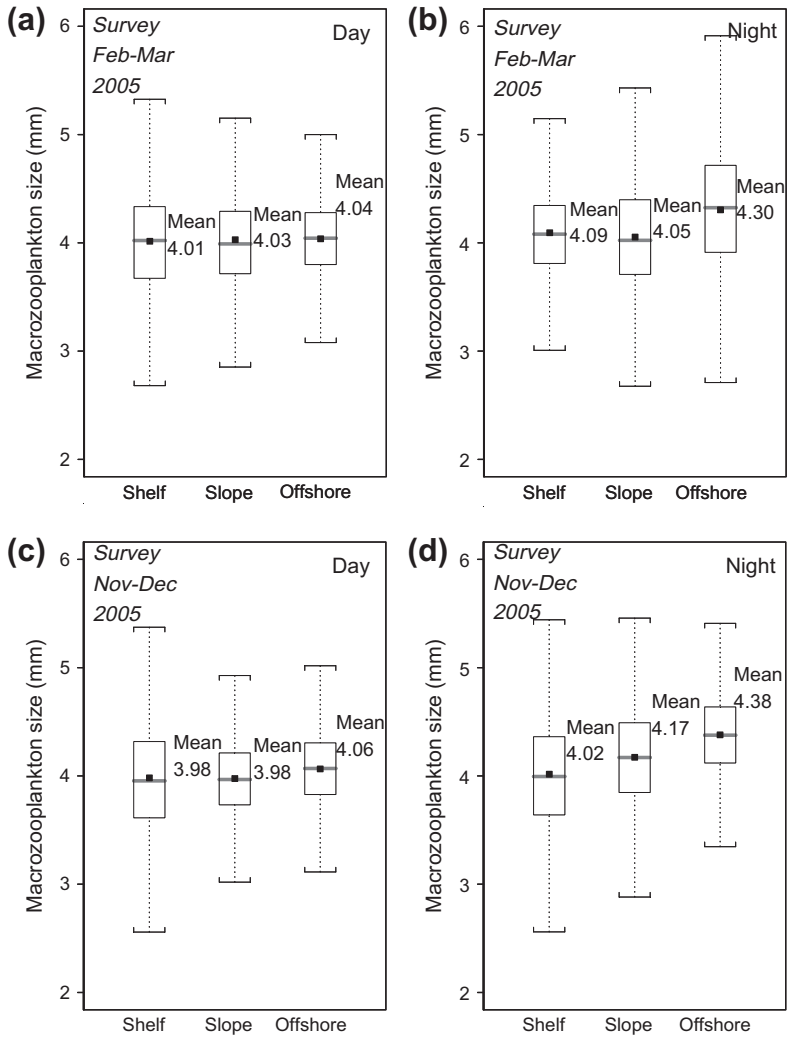

Fig. 8. Day and night box plots of epipelagic macrozooplankton ESR (in mm) according to the shelf, slope and the offshore ecological domains for both Austral summer (a and b) and spring (c and d) 2005 (for details on box plot see the caption of Fig. 5).

3.5. Along-shore macrozooplankton biomass and size distribution

Patterns of along-shore macrozooplankton biomass distribution varied according to the diel period and the survey. During the day, low macrozooplankton biomass dominated in all latitudes without exhibiting any clear along-shore pattern. During the night, higher macrozooplankton biomasses were observed in the northern and southern areas, coinciding with the area where the continental shelf was narrower (Fig. 11b and d). The pattern, however, did not persist when separating the macrozooplankton data according to the shelf, slope and offshore (figures not shown). This separation revealed that the apparent along-shore pattern was an artefact of the sampling design, which did not sample the ecological domains with the same intensity.

Similar along-shore distribution patterns were observed between macrozooplankton biomass and sizes, with larger sizes coinciding with high biomass (Figs. 11 and 12).

3.6. Macrozooplankton horizontal distribution

The maps of horizontal epipelagic macrozooplankton biomass distribution constructed from acoustic data and Hensen net sampling data (integrated over the 50 upper metres) exhibited overall similar spatial patterns (Figs. 13 and 14). In particular the increase in macrozooplankton biomass toward offshore was evidenced from both data sources. This pattern was particularly noticeable during the night but also observable during the day. However, macrozooplankton from the acoustic survey displayed a greater biomass difference between day and night when compared to that from net sampling, in particular in the offshore area. In addition, some hot spots (e.g. extreme north in austral summer 2005 and offshore at ~13°S in austral spring 2005) were detected by both acoustic and net data. Since there is about three orders of magnitude more acoustic data than net-sampled data, the interpolated maps of macrozooplankton biomass from acoustic data also provided far more details on macrozooplankton patchiness which could not be detected from net data.

4. Discussion

This study provides the first direct estimation of macrozooplankton biomass in the NHCS. We will first discuss the validity of our method and determine which organisms are mainly responsible of the observed acoustic distribution pattern. Then we will compare our macrozooplankton biomass estimations with other estimations from the same and other systems. Finally, we will discuss how these new findings allow for a better understanding of the high fish productivity in the NHCS.

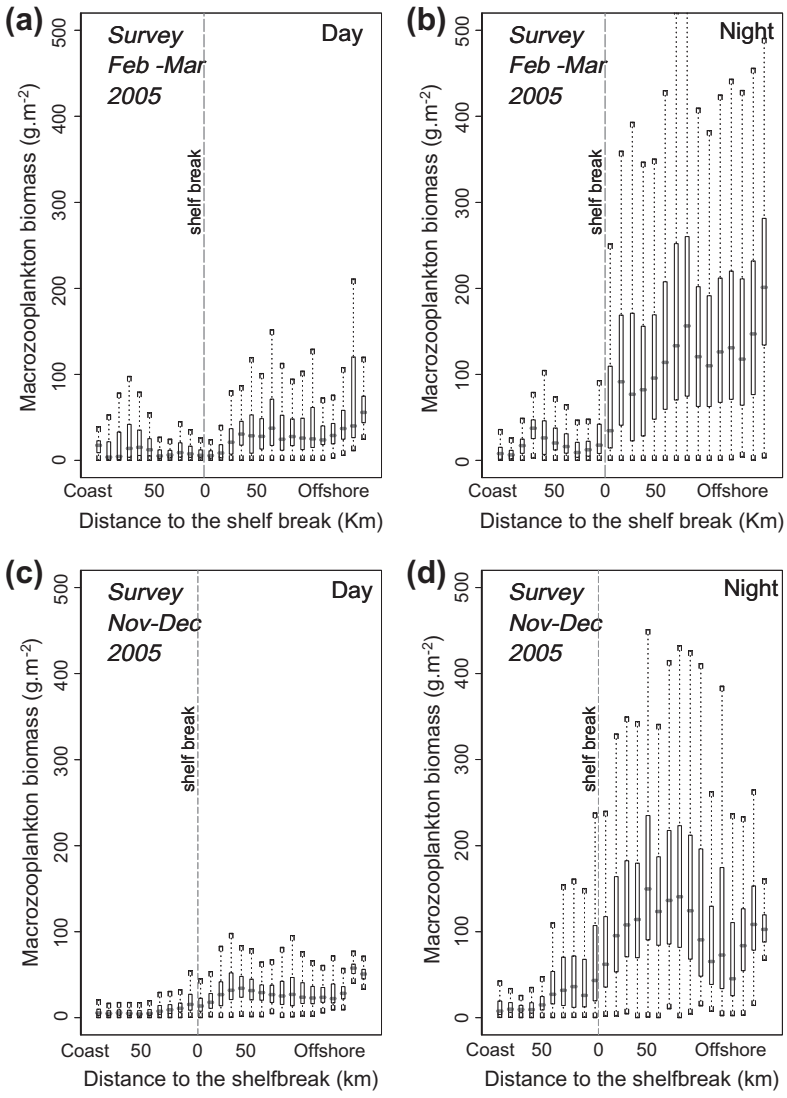

Fig. 9. Day and night box plots of across-shore macrozooplankton biomass (g m^{-2}) in relation to the shelf break for both Austral summer (a and b) and spring (c and d) 2005(for details on box plot see the caption of Fig. 5).

4.1. Validation

The main difficulty in validating the acoustic results resides in the availability of independent observations. Nets are the most common tool used to sample marine pelagic organisms. Unfortunately, the confidence in net biomass estimation can be low or high depending on the type of net and the target species. Beside these limitations, our results demonstrate that the discrimination between scatterers is correct, as the patterns of vertical and horizontal distribution of acoustic biomass of fish, squat lobster and fluid-like macrozooplankton agreed with the independent observation from net sampling. Fish discrimination was not a challenge since IMARPE is performing accurate acoustic fish biomass estimation (from a single frequency) validated with ground-truthed catch data for decades (Simmonds et al., 2009). Also squat lobster, with some limitation, is routinely assessed by IMARPE (since 1998, Gutiérrez et al., 2008) using a single frequency. The difficulty arises when squat lobster and anchovy occur in the same vertical layer (Bertrand et al., 2008; Gutiérrez et al., 2008), particularly during the night. Although a bi-frequency method has previously been used to separate anchovy and squat lobster (Bertrand et al., 2008), our study is the first one providing a detailed and validated acoustic method for separating these two organisms in the NHCS. In addition to trawl sampling ground-truthing, visual examination of echograms qualitatively confirmed the robustness of the capacity for discrimination of the method.

The challenge we faced concerned mainly the fluid-like category. Our results showed that acoustic fluid-like vertical and horizontal patterns of biomass distribution were very similar to that of the euphausiids, the main macrozooplankton group in the system (Ayón et al., 2008a; Espinoza and Bertrand, 2008). Still, there was one order of magnitude difference between fluid-like acoustic and multinet biovolumes. However, it is well known that macrozooplankton avoid net sampling (Debby et al., 2004). This avoidance is attributed to both visual and mechanical disturbances and usually increases when smaller nets are used (Fleminger and Clutter, 1965). According to Brinton (1967), euphausiids display a stronger avoidance at the surface as the higher illumination might allow them to detect the net. The effect can be exacerbated by using vertical samplings with nets with small open areas mouth, as is the case of the Hansen and multinet systems used in the NHCS. However, the similarity of euphausiid and acoustic fluid-like patterns and the apparent ability of euphausiids to avoid nets, do not themselves constitute a validation of the biovolume difference

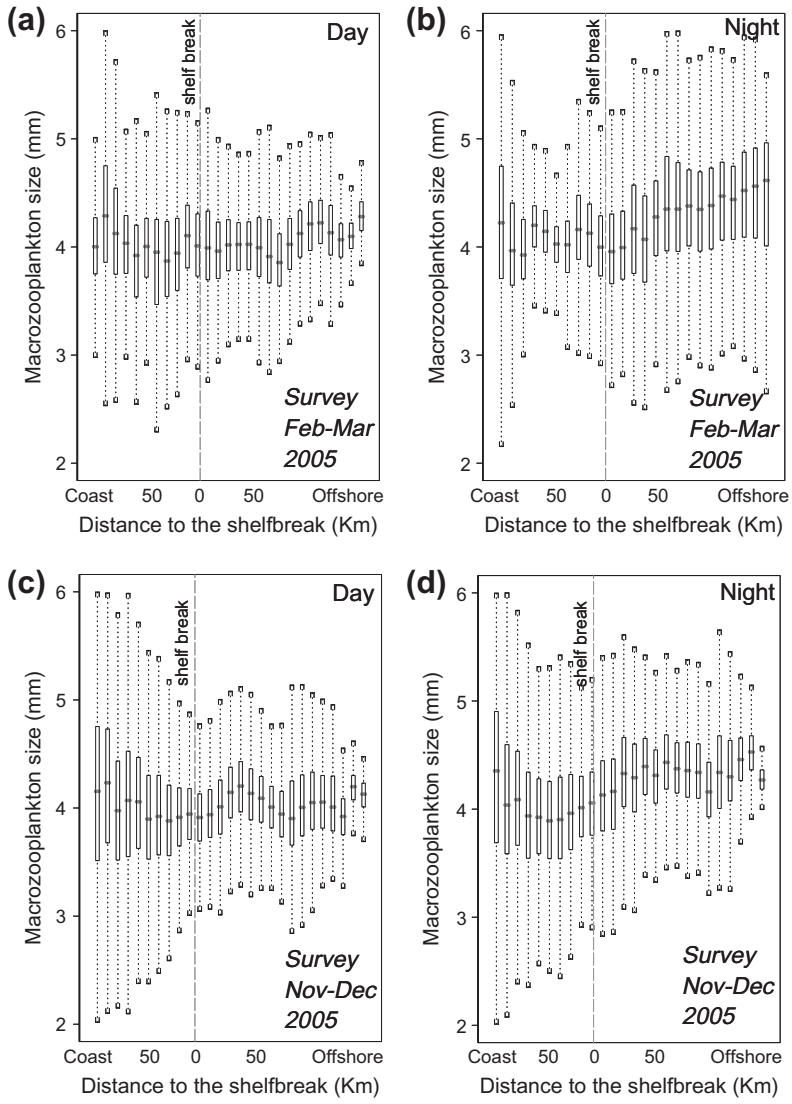

Fig. 10. Day and night box plots of across-shore zooplankton ESR (in mm) in relation to the shelf break for both Austral summer (a and b) and spring (c and d) 2005 (for details on box plot see the caption of Fig. 5).

between the nets used and the acoustic method, since the only way to assess the catching power of any net is to compare it to a larger net. This is a work that needs to be performed in the NHCS.

Moreover, notwithstanding the apparent importance of euphausiids in the fluid-like acoustic patterns, it is worth noting that the acoustic biovolume also includes other organisms with considerable biomass such as large copepods.

Finally, the blue-noise acoustic field could not be validated as this field is a kind of 'black box' supposed to be composed by organisms that are difficult to sample (e.g. gelatinous organisms, fish larvae).

4.1.1. Day–night difference

The high day–night difference in the estimated epipelagic biomass illustrates the fact that the bulk of the nocturnal epipelagic biomass is composed of migratory fluid-like macrozooplankton. By definition, migratory organisms were not included within the epipelagic biomass during the day. The direct biomass estimation of these organisms was not possible by day because they migrate deeper than the actual acoustic range of the Simrad EK500 at 120 kHz, which we used in this study (150 m). It is worth mentioning that data acquired during the 'Filamentos 2008' survey with the Simrad EK60 at 120 kHz (permitting work down to 300 m) showed that most of the migrating macrozooplankton community formed a layer at about 200 m during the day (see Fig. 9). We could estimate the biomass of migrating macrozooplankton by subtracting the diurnal estimation from the nocturnal, which encompass both migrating and non-migrating communities. We found that ~79% of the macrozooplankton observed during the night performed vertical migration. This result is similar to the estimations provided by Escribano et al. (2009) in the Southern HCS (75%) and Postel et al. (2007) in the Northern Benguela system (71%). In the Southern HCS, Escribano et al. (2009) also found that the main constituent of the biomass of this migratory community was large zooplankton, mainly euphausiids but also large *Eucalanus* spp. copepods. In this study we have found that macrozooplankton size increased about 5% during the night. This suggests that the migratory fluid-like macrozooplankton not only attained a much higher biomass than the non-migrating community but is also composed of larger individuals.

4.1.2. Across- and along-shore distribution of macrozooplankton

In this study, migratory macrozooplankton composed of relatively large organisms was more abundant over the slope and the

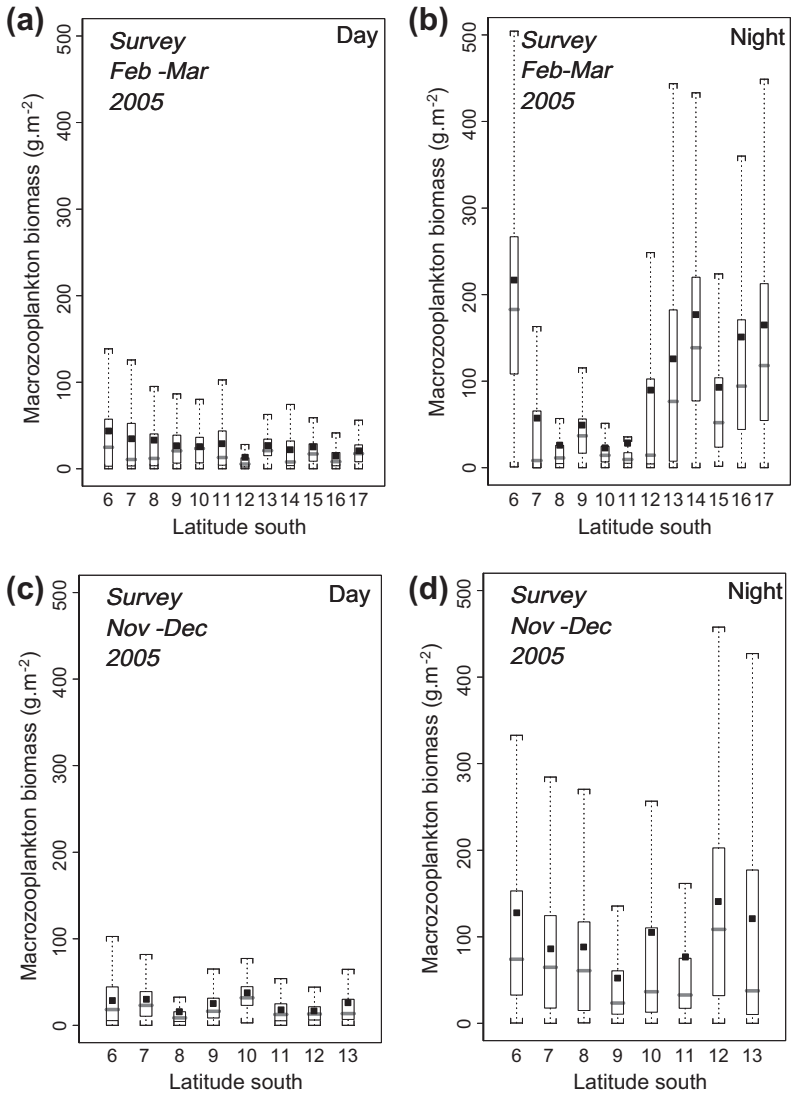

Fig. 11. Day and night box plots of along-shore macrozooplankton biomass distribution (g m^{-2}) for both austral summer (a and b) and spring (c and d) pelagic surveys of 2005. Box plots were constructed by intervals of one degree of Latitude (for details on box plot see the caption of Fig. 5).

offshore domain. This pattern was also observed in the along-shore macrozooplankton distribution. Lower biomass and smaller size were estimated in the latitudes with a relatively wide continental shelf; in contrast, higher biomass and larger size were estimated in the latitudes with narrower continental shelf (Ayón et al., 2008a). The high biomass of this migratory macrozooplankton was apparently delimited by the shelf break. The shelf break is known to play an important role in transporting and retaining zooplankton (Bakun, 1996; Genin, 2004; Zhu et al., 2009). Shelf break upwelling can result from the interaction between subsurface currents and the shelf break (Hill and Johnson, 1974; Lill, 1979; Bakun, 1996). To counteract the upslope upwelling transport toward the surface, it has been suggested that euphausiids swim downward against the upwelling during day which allows them to keep a preference depth (Genin, 2004). This would result in a retention and accumulation of euphausiids along the shelf break (Genin, 2004). Thus, a very high concentration of euphausiids usually occurs where the deep flow is convergent and the upwelling is the strongest (Simard and Mackas, 1989; Mackas et al., 1997). An ecological advantage of this counter-upwelling swimming behaviour of euphausiids would be the ability to stay near the shelf break upwelling and exploit the enhanced phytoplankton productivity and biomass during the night migration to the surface (Lu et al., 2003). In the NHCS there is a lack of knowledge about euphausiid distribution (Ayón et al., 2008b); information from other upwelling regions, however, has shown that euphausiid distribution is strongly affected by the shelf break (Barange and Pillar, 1992; Swartzman et al., 2005). In the California Current system, euphausiid patches are more frequently observed along the shelf break over the slope area (Swartzman et al., 2005). In the Benguela system, the shelf break seems to effectively separate inshore and offshore euphausiid populations which complete their life cycles within each area (Barange and Pillar, 1992). In the Canary system, there is also evidence of higher euphausiid abundance off the shelf break, in the slope area (Blackburn, 1979). Thus, the observed across-shore pattern of macrozooplankton in this study, together with the evidence of high euphausiid densities over the slope and offshore area (Vinogradov and Shushkina, 1978), suggest that the shelf break might also be important for retaining and accumulating macrozooplankton over the slope and offshore areas of the HCS.

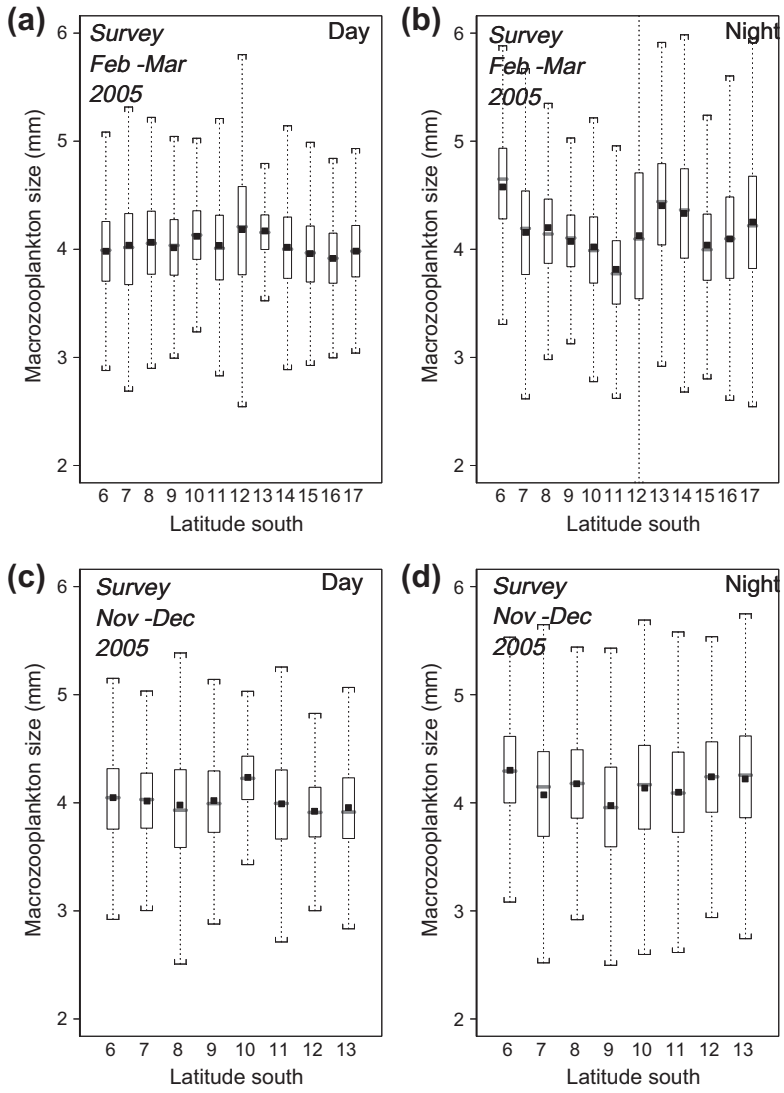

Fig. 12. Day and night box plots of along-shore macrozooplankton ESR distribution (mm) for both Austral summer (a and b) and spring (c and d) pelagic surveys of 2005. Box plots were constructed by intervals of one degree of Latitude (for details on box plot see the caption of Fig. 5).

4.1.3. Matching the fluid-like horizontal patterns to specific macrozooplankton taxa

Despite the lack of ground-truthed catch data to effectively allocate this high nocturnal biomass to macrozooplankton taxa (multinet data were only available during the surveys 'Cardumenes 2004' and 'Filamentos 2008' and Hensen zooplankton data are available as global biovolume and not discriminated by taxonomic group), only few macrozooplankton organisms could reach such a high biomass and/or fit the patterns described above: squat lobster, salps, large copepods and euphausiids. Squat lobster has been separated from other fluid-like organisms based on a threshold S_v value. Squat lobster echoes with low S_v could have been misclassified as macrozooplankton leading to an overestimation of its biomass. This species, however, is vertically constrained within the epipelagic zone and does not perform large vertical migrations. In addition, Gutiérrez et al. (2008) showed that squat lobster distribution is restricted to the coldest (coastal) part of the cold coastal water. Thus squat lobster is mainly confined to the shelf area; an area in which the estimated macrozooplankton biomass was lower. Although squat lobster larvae cannot be distinguished as an independent fluid-like group, their high abundance could only have contributed to the macrozooplankton biomass in near-coastal areas (Fagetti and Campodonico, 1971). Salps can reach high biomass and are capable of migrating vertically (Pakhomov, 2004). However, these organisms are mainly distributed in equatorial and tropical waters that are restricted to the northern part of NHCS (Ayón et al., 2008a), an area that was excluded from this study. We can thus assume that salps account only for a minor part of the estimated macrozooplankton biomass.

Large copepods, in particular *Eucalanus inermis*, are relatively abundant in the system (Ayón et al., 2008a) and are the second most important food item of anchovy and sardine (Espinoza and Bertrand, 2008; Espinoza et al., 2009). *E. inermis* also perform large diel vertical migration between the epipelagic layer and the OMZ (Ayón et al., 2008a; Escribano et al., 2009). These large copepods, however, need to occur at a very high density to be properly detected and quantified by the used acoustic frequencies (Murase et al., 2009) even if the +MVBS method should improve the acoustic power of detection thanks to a better discrimination (Lebourges-Dhaussy and Fernandes, unpublished data). *E. inermis* is considered a typical zooplankton of the cold coastal water and used as indicator for the presence of this water mass (Ayón et al.,

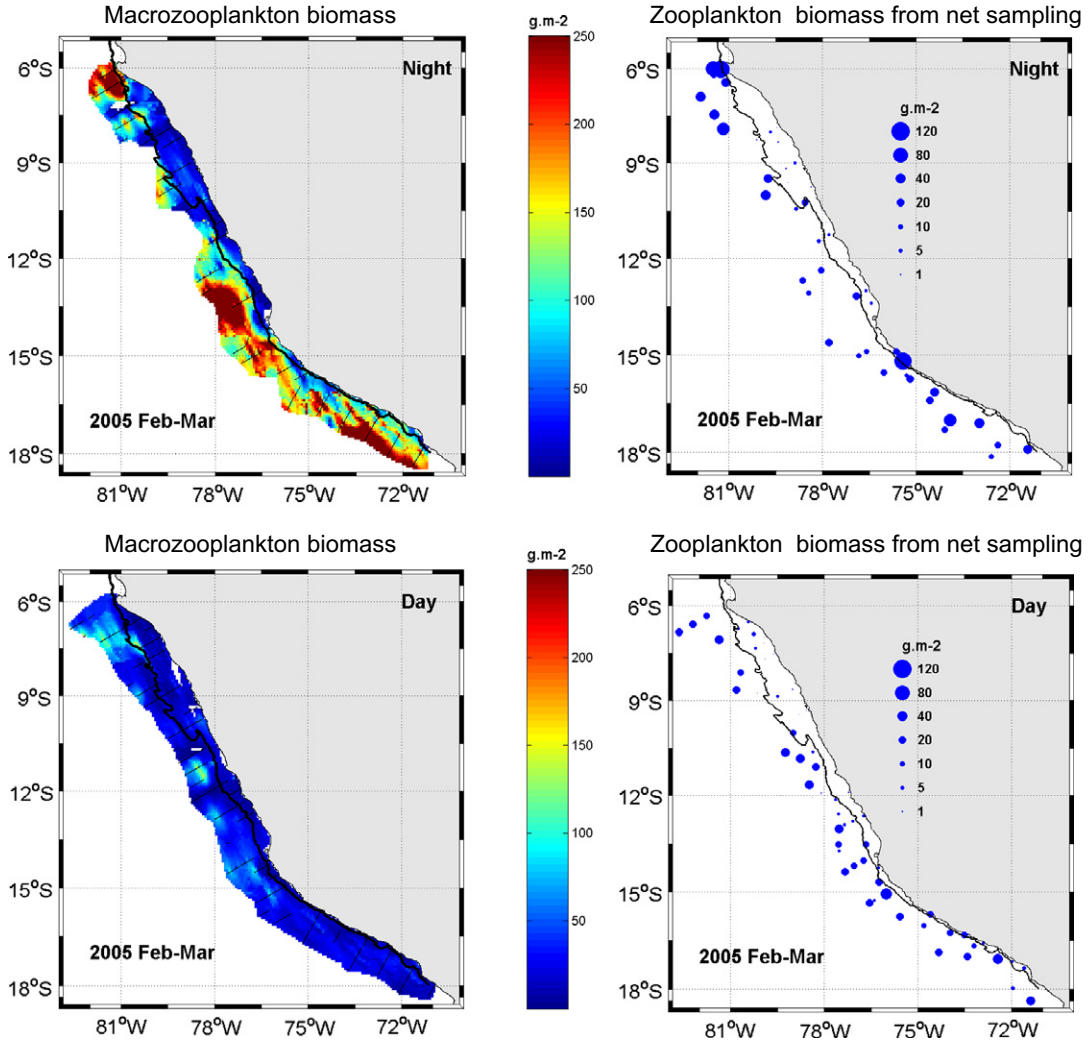

Fig. 13. Horizontal zooplankton biomass (g m^{-2}) distribution during Austral summer 2005. Acoustic macrozooplankton biomass of the epipelagic community during day (a) and night (c). Zooplankton biomass from Hensen nets towed vertically from 50 m to the surface during day (b) and night (d). The black line shows the continental shelf limit (200 m bottom depth).

2008a). Thus high densities of *Eucalanus* spp. are more likely to occur in and contribute to the macrozooplankton biomass in the shelf area rather than in offshore areas.

Finally, euphausiids, particularly the endemic species *Euphausia mucronata*, which constitute up to 50% of the total system zooplankton biomass (Antezana, 2002), present a similar distribution pattern to the one described in acoustic data. Euphausiid species are adapted to the OMZ and can stand very low dissolved oxygen concentration (Antezana, 2002, 2010; Escribano et al., 2009). They perform extensive diel vertical migration from the photic zone, where they forage during the night, to the OMZ, where they take refuge during the day (Escribano et al., 2009). Adults are usually distributed offshore where they can reach a very high biomass (Vinogradov and Shushkina, 1978; Escribano et al., 2009) while juvenile and larvae are usually distributed in the shelf area (Aronés et al., 2009). Also, the high biomass of euphausiids is indirectly confirmed by anchovy, sardine and jack mackerel diets (Konchina, 1981, 1991; Espinoza and Bertrand, 2008; Espinoza et al., 2009). The proportion of euphausiids in anchovy diet is higher offshore during the night (P. Espinoza, IMARPE, unpublished data). The similarities between the nocturnal patterns of size and macrozooplankton biomass distribution from this study and the known patterns of euphausiids, in particular *E. mucronata*, suggest that euphausiids are the main constituent of the acoustic macrozooplankton biomass estimated during night.

In this study we also found large fluid-like organisms with relatively low biomass near the coastal areas. Near-coastal areas usually contain a distinct zooplankton community in which meroplanktonic larvae of benthic invertebrates (e.g. decapoda, cirripedia, mollusca, polychaeta) constitute an important part (Criales-Hernández et al., 2008). Moreover, the large larvae of squat lobster, the most abundant and largest macrozooplankton within the cold coastal water (Gutiérrez et al., 2008), may be quite abundant near the coast (Fagetti and Campodonico, 1971). This highly diverse near-coastal zooplankton community is therefore more likely to contain larger organisms than the inner shelf community, which is composed mainly of copepods (Ayón et al., 2008a), which could explain the observed large fluid-like size in the near-coastal areas.

In summary our macrozooplankton biomass estimation potentially includes a variety of fluid-like organisms such as misclassified adult squat lobster, juvenile squat lobster, salps, large copepods, meroplanktonic crustacean larvae and euphausiids. However, when contrasting organism behaviour and habitat preferences with the observed day–night differences in fluid-like biomass and size, along with the across- and along-shore fluid-like

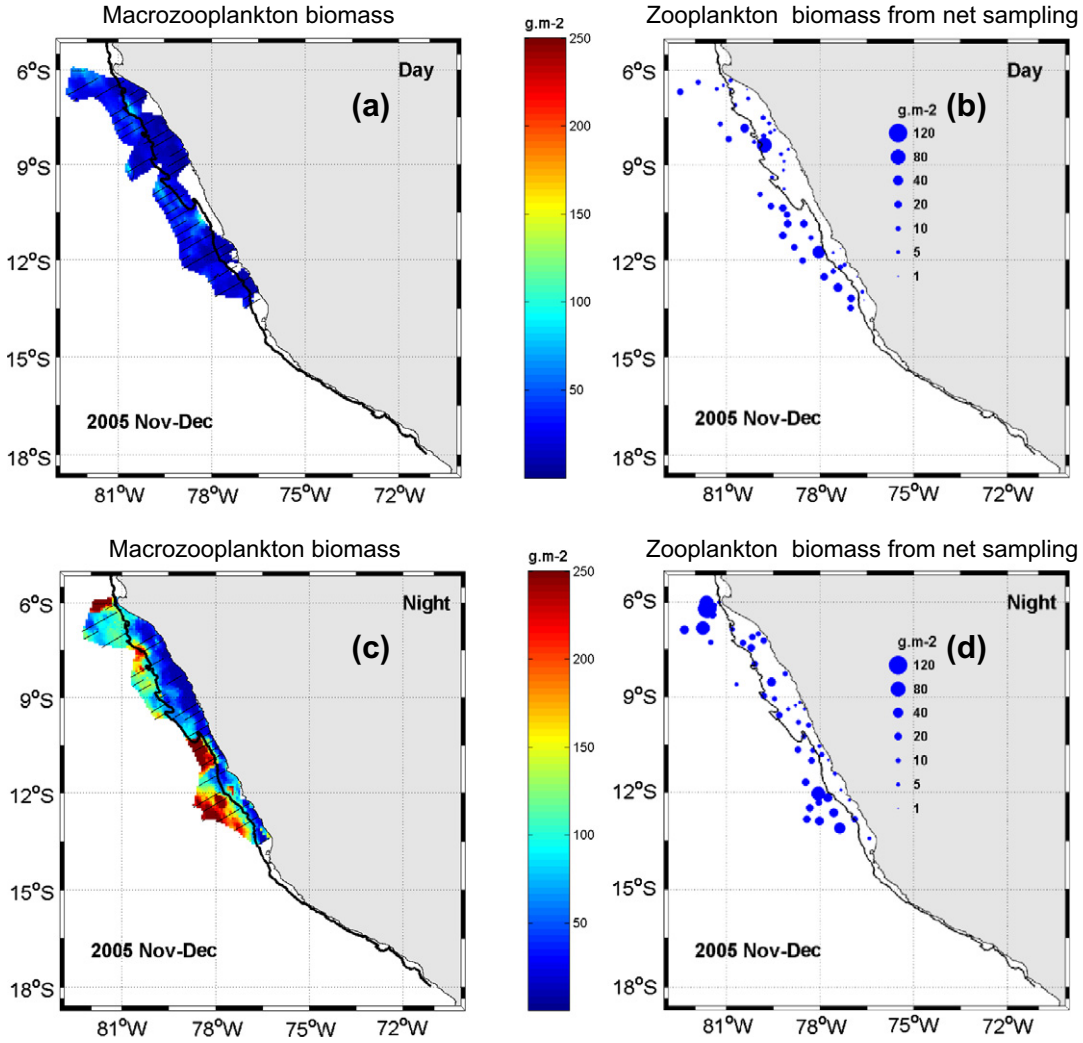

Fig. 14. Horizontal zooplankton biomass (g m^{-2}) distribution during Austral spring 2005. Acoustic macrozooplankton biomass of the epipelagic community during day (a) and night (c). Zooplankton biomass from Hensen nets towed vertically from 50 m to the surface during day (b) and night (d). The black line shows the continental shelf limit (200 m bottom depth).

distribution, euphausiids are probably the main constituent of the fluid-like group observed in acoustic data even if other fluid-like scatterers probably account for a significant part of the fluid-like group.

4.2. Macrozooplankton biomass in the NHCS: higher than assumed

This study provides the first direct high-resolution large-scale estimation of macrozooplankton biomass in the NHCS and it is to our knowledge the first one from any of the main upwelling systems. The total estimated biomass, i.e., the biomass estimated during the night when both migrating and non-migrating macrozooplankton communities are in the epipelagic layer (~105 g m^{-2}), was more than five times higher than their corresponding net sampling of total zooplankton biomass (~21 g m^{-2}). This high difference is not surprising, since macrozooplankton usually avoid nets (Fleminger and Clutter, 1965; Debby et al., 2004), which results in an underestimation of global zooplankton biomass by net sampling when compared to acoustics (Lawson et al., 2008). The use of the density (g) and sound speed (h) contrast parameters from *Euphausia pacifica* instead of from *E. mucronata* may also introduce some bias, since these parameters tend to vary between both different environmental conditions and different species (Smith et al., 2010). The g and h parameters were used to estimate the macrozooplankton target strength and abundance, the estimation of which is quite sensitive to even small differences in contrast parameters (Stanton and Chu, 2000; Smith et al., 2010). As there are no measurements of g and h parameters of any macrozooplankton species of the HCS, it is not yet possible (acoustically) to know if we have over- or underestimated macrozooplankton biomass. However, since the estimated biomass from this study is among the lowest that could result from using current g and h parameters available in the literature (Greenlaw and Johnson, 1982; Chu and Wiebe, 2005; Smith et al., 2010), the probability of overestimating the macrozooplankton biomass seems low.

Furthermore, since macrozooplankton (particularly euphausiids) are cylindrical rather than spherical, as assumed in our backscattering model, additional uncertainty in the biomass estimates could have been introduced because of this assumption. Although this bias may be reduced in this study because we (i) restricted inference to macrozooplankton biovolume (Holliday and Pieper, 1995), (ii) worked with averaged echoes, thus smoothing individual behaviour, and (iii) restricted analysis to true day and nighttime data, excluding migratory periods and thus increasing the chance of including broadside incidence in the range of animal

orientation (Stanton and Chu, 2000), further studies are needed to unveil and quantify these effects in our biomass estimates.

Therefore, there is still concern about the accuracy of the acoustic method: is this a realistic estimation of the macrozooplankton biomass of the NHCS?

The ideal situation would be to compare our results with validated acoustic estimates from the same system and from other comparable upwelling systems. However, most of the studies that provided biomass acoustic estimates have been performed in the Antarctic area, where acoustics is used as a standard tool to estimate krill biomass (Watkins and Brierley, 2002). Acoustics has seldom been used in eastern boundary upwelling systems (EBUS) to estimate zooplankton biomass (Ressler et al., 2005; Postel et al., 2007). When employed, acoustics was calibrated to match the biomass levels obtained by net sampling (Ressler et al., 2005; Postel et al., 2007) and was not used to provide independent biomass estimates. In EBUS, only net sampling and trophic model estimations are available to compare our results. To facilitate the comparison and the discussion, we synthesised the published zooplankton biomass estimation in EBUS, Antarctica and Eastern Canada (Table 2). These estimates were obtained from different nets and mesh sizes taken over various vertical ranges, from trophic models and from acoustics. Thus, each individual estimate corresponds to a set of different conditions and must be taken with caution when used as a reference value for the purpose of comparison.

4.2.1. Comparing with in situ data (net and acoustic)

Compared with all biomass estimations considered in Table 2, our estimates are among the highest and generally more than twice as high as others estimates. Comparable or higher biomass estimates were encountered only in some specific measurements in the southern HCS (Escribano et al., 2009, from only four net samples), the Northern Benguela during the 1960s (Cushing, 1971), Canada (Cotte and Simard, 2005) and Antarctica.

The only work that compared zooplankton biomass (from net samples) between upwelling systems is a synthesis from Cushing (1971). According to Cushing (1971) zooplankton biomass was about 40–50 g m^{-2} in all EBUS. Lower biomasses were observed in southern California (21 g m^{-2}) and in the southern Humboldt Current (~33 g m^{-2}), higher biomasses were observed in northern Canary system (21°N–28°N, 80 g m^{-2}) and northern Benguela (23°S–29°S, 114 g m^{-2}), while intermediate biomasses (~50 g m^{-2}) were estimated in the NHCS. Our estimation ranges among the highest values proposed by Cushing (1971) but is more than twice as high as most other cases. Cushing estimates come from different sources and net types that may partly limit the comparison. Also, Cushing (1971) assumed that the zooplankton biovolume was mainly composed of crustacean zooplankton and converted this biovolume into biomass without excluding or correcting the contribution of tunicates (salps), which may have led to an overestimation of this biomass (Lavaniegos and Ohman, 2007).

4.2.2. Comparing with trophic models and what we know about trophodynamics

Macrozooplankton abundance and/or their turn-over rates can be indirectly determined by trophic models. These models estimate the amount of prey biomass required to balance its predator consumption. The availability of diet information is crucial when building trophic models and any misevaluation of a predator's diet would definitely affect prey biomass estimates, particularly if the predators attain very high biomasses, as is the case of anchovy. So far, trophic models constructed in the NHCS have considered that anchovy forage mainly on phytoplankton or to the same extent on phytoplankton and zooplankton (e.g. Jarre-Teichman, 1992; Tam et al., 2008). Since we now know that this is not the case (Espinoza and Bertrand, 2008; Espinoza et al., 2009), we can assume that these trophic models strongly underestimated zooplankton, particularly macrozooplankton, biomass.

In addition to diet information, a trophic model needs to be based on how fast a prey population produces its own biomass in a given time. In other words, it requires the prey production/biomass ratio (P/B). Since predators' consumption can be balanced by combining low prey biomass with high P/B ratios, or vice versa, it is advisable to look at the assumed P/B ratios. To build trophic models of the NHCS, Tam et al. (2008) and Guénette et al. (2008) used a P/B of 20 for the macrozooplankton (euphausiids). The P/B ratio of euphausiids from similar environments usually ranges between 9 and 15 (Taki, 2006). Thus, the apparent high ratio assumed by the trophic models in NHCS also led to an underestimation of macrozooplankton biomass.

In the NHCS, anchovy biomass has been estimated to 83 g m^{-2} (period 1995–1996, Tam et al., 2008). This biomass is 50% higher than our macrozooplankton biomass from the anchovy distribution area (~55 g m^{-2}), but 21% lower than the total macrozooplankton biomass estimation (~105 g m^{-2}). The comparison of these predator and prey biomasses recalled the main question of this study: are these prey biomasses large enough to feed the anchovy population? To provide an answer, we needed to determine if macrozooplankton production could fit with the predation from anchovy and other main predators (Tam et al., 2008) when using our macrozooplankon biomass estimation, appropriate predator diets (Espinoza and Bertrand, 2008; Espinoza et al., 2009) and predator consumption ratios (Guénette et al., 2008). We found that for the overlapped area between fish and macrozooplankton (55 g m^{-2}), a high P/B ratio of 21 had to be assumed to produce enough macrozooplankton production to feed anchovy (83 g m^{-2}) and other predators (~27.6 g m^{-2}). For the total area, however, the assumed P/B ratio (11) lay within the expected values of euphausiids from environments similar to the NHCS (Taki, 2006). This suggests that either there is an underestimation of macrozooplankton biomass or that there is a 'continuous' supply of macrozooplankton biomass from richer non-overlapped areas (offshore). It is known that anchovy population is restricted to the coastal area and generally occupies less than 154,000 km^2 (Gutiérrez, 2000; Simmonds et al., 2009), while the distribution of euphausiids and other main macrozooplanktonic species occupy a much larger area (Brinton, 1962). The total biomass of macrozooplankton estimated in the study area (105 tonnes km^{-2} * 263,000 km^2) is actually 2.2 times that of anchovy (83 tonnes km^{-2} * 154,000 km^2), which probably helps to compensate for the grazing effect in areas of overlap between fish and macrozooplankton.

To successfully achieve a life cycle closure in an upwelling system, macrozooplankton species must be adapted to the offshore drift of surface waters and the onshore flow of upwelling source water (Peterson, 1998). For instance, the ontogenetic vertical migration of some main macrozooplankton species, such as *Eucalanus inermis* and *Euphausia mucronata* (Escribano et al., 2009), might allow them to counterbalance the surface advection of early life stages by increasing the range of dial vertical migration (DVM) and thus reaching subsurface layers dominated by onshore transport (Mathisen, 1989; Brochier et al., 2008). We suggest that the ontogenetic vertical migration of macrozooplankton can also help to bring a fresh supply of biomass to the depleted inshore areas. In addition, fish shoals rove around in the upper layer moving in the order of 10–20 km per day and feeding intensively on macrozooplankton which migrate upwards during the night from the OMZ layer. Since macrozooplankton and fish may be moving in different directions, every night there is a 'refreshing' of the food supply for the aggregation of the shoal groups which characterise the distribution of Peruvian anchoveta.

In summary, our estimation of macrozooplankton biomass seems coherent because it (i) is about five times higher than the

Table 2
Synthesis of biomass estimations (in g m^{-2}) of meso- and macrozooplankton in main upwelling systems, Antarctic and eastern Canada.

Region	Sampling method	Depth sampled (m)	Sampling date	Mesozooplankton	Macrozooplankton	Time	Reference and comments
Humboldt Northern 6°–18°S	Acoustic, this study	Z_{VEEP}	February–March 2005		28.6	Day	This study
					114.6	Night	This study
Humboldt Northern 6°–13°S	Acoustic, this study	Z_{VEEP}	November–December 2005		24.3	Day	This study
					112.4	Night	This study
Humboldt Northern 4°–18°S	Hansen net 300 μm/0.33 m^2	Upper 50	February–March 2005	12.9		Day	This study
				21.2[a]		Night	
	Hansen net 300 μm/0.33 m^2	Upper 50	November–December 2005	13.8		Day	
				22.1[a]		Night	
Humboldt Northern 4°–18°S	Hansen net 300 μm/0.33 m^2	Upper 50	Austral summer 1960s	39.9[a]			Ayón et al. (2004). Conversion from biovolume to wet weight. Factor from Wiebe et al. (1975) and Wiebe (1988)
	Hansen net 300 μm/0.33 m^2	Upper 50	Austral summer 1970s	24.7[a]			
	Hansen net 300 μm/0.33 m^2	Upper 50	Austral summer 1980s	10.9[a]			
	Hansen net 300 μm/0.33 m^2	Upper 50	Austral summer 1990s	17.1[a]			
Humboldt Northern 4°–10°S	Diverse	Upper 300	1960s	51.5[a]			Cushing (1971). Conversion from gC m^{-2} to wet mass g m^{-2} from Hunt et al. (1981)
Humboldt Northern 10°–18°S	Diverse	Upper 300	1960s	45.5[a]			Cushing (1971). Conversion from gC m^{-2} to wet mass g m^{-2} from Hunt et al. (1981)
Humboldt Northern 4°–16°S	Trophic model		1995–1996	31.2	21.1		Tam et al. (2008). Macrozooplankton P/B ratio assumed to be 20. Period 1997–1998 correspond to a very strong El Niño. Area within 60 nm from the coast
	Trophic model		1997–1998	17	34.8		
Humboldt Northern 4°–14°S	Trophic model		1953–1984		50		Guénette et al. (2008). Macrozooplankton P/B ratio assumed to be 20. Area within 40 nm from the coast. Anchovy diet 0.3 diatom and 0.6 macrozooplankton
Humboldt Southern 33°–39°S	Trophic model		1992	48.9	73.6		Neira et al. (2004). Only to meet the energy demand of the commercial fish sp. Low P/B ratio for macrozooplankton (2.6).
			1998	70.8	106.3		
Humboldt Sourhern 20°S	Tucker trawl net 300 μm/1 m^2	Upper 60	March 2000		64.1	Day	Escribano et al. (2009). Epipelagic layer offshore area from 4 stations.
					355.9	Night	
Humboldt Southern 36°30′S	Tucker trawl net 200 μm/1 m^2	Upper 80	August 2002 to December 2005	46.6		Day	Escribano et al. (2007). One coastal station over time for 3 years 2002–2005. Conversion from mgC m^{-2} to wet mass g m^{-2} from Hunt et al. (1981)
Humboldt Southern 23°–35°S	Diverse	Upper 300	1960s	34.2[a]			Cushing (1971). Conversion from gC m^{-2} to wet mass g m^{-2} from Hunt et al. (1981)
Humboldt Southern 35°–45°S	Diverse	Upper 300	1960s	33.2[a]			Cushing (1971). Conversion from C m^{-2} to wet mass g m^{-2} from Hunt et al. (1981)
California Central 35°–38°N	Double oblique tows using ring (1 m diameter) and bongo net (0.71 m diameter) ~0.5 mm mesh size	Upper 140–210	1951–2005	6.7	3	Night	Lavaniegos and Ohman (2007). Converted from organic carbon to wet weight from Hunt et al. (1981)
California Southern 31°–34°N	Double oblique tows using ring (1 m diameter) and bongo net (0.71 m diameter) ~0.5 mm mesh size	Upper 140–210	1951–2005	5.9	1.4	Night	Lavaniegos and Ohman (2007). Converted from organic carbon to wet weight from Hunt et al. (1981)
California Southern 31°–34°N	Diverse	Upper 140	1960s	21.2			Cushing (1971). Conversion from C m^{-2} to wet mass g m^{-2} from Hunt et al. (1981)
California Central 34°–40°N	Diverse	Upper 140	1960s	43.5			Cushing (1971). Conversion from C m^{-2} to wet mass g m^{-2} from Hunt et al. (1981)

(*continued on next page*)

Table 2 (*continued*)

Region	Sampling method	Depth sampled (m)	Sampling date	Mesozooplankton	Macrozooplankton	Time	Reference and comments
California Northern 40°–48°N	Diverse	Upper 140	1960s	53			Cushing (1971). Conversion from C m^{-2} to wet mass g m^{-2} from Hunt et al. (1981)
Benguela Northern 9°–20°19′S	L-ADCP calibrated by multinet	Upper 200	September 2000	39.8[a] 11.5[a]		Night Day	Postel et al. (2007). Converted from ash freedry mass to dry mass by factor 0.8^{-1} (Postel et al., 2000) and from dry mass to wet mass by factor 0.1^{-1} Hutchings et al. (1991)
Benguela Northern 15°–29°S	Trophic model			11.7	8.2		Heymans and Baird (2000). Converted from organic carbon to wet weight from Hunt et al. (1981)
Benguela Northern 17°30–26°S	Bongo net 300 and 500 μm mesh size	Upper 50	September and November 1982 January–March, September and November 1983January and March 1984		32.8	Night	Barange and Stuart (1991). Only biomass of *Nyctiphanes capensis* (94%) and *Euphausia hanseni* (6%). Converted from dry mass to wet mass by factor 0.1^{-1} from Hutchings et al. (1991)
Benguela Southern South of 29°S	Trophic model		1980s	8.0	13.3		Shannon et al. (2003). Biomass required to sustain the other components of the system. Macrozooplankton P/B ratio was assumed to be 13 (from Hutchings et al., 1991)
			1990s	8.7	14.6		
Benguela Northern 17°–23°S		Upper 200	1960s	56.9			Cushing (1971). Conversion from C m^{-2} to wet mass g m^{-2} from Hunt et al. (1981)
Benguela Northern 23°–29°S		Upper 200	1960s	113.8			Cushing (1971). Conversion from C m^{-2} to wet mass g m^{-2} from Hunt et al. (1981)
Benguela Southern 29°–34°S		Upper 200	1960s	48.5			Cushing (1971). Conversion from C m^{-2} to wet mass g m^{-2} from Hunt et al. (1981)
Canary Current along a line at 21°40′N,	Bongo net 102 μm mess size	Upper 200	March, April, May 1974	3.5[a], 10.5[a] and 76.2[a]	16–208	Night	Blackburn (1979). Biomass from the inner shelf, outer shelf and slope respectively. Macrozooplanton biomass made up 79% of the slope biomass (76.2)
Canary Current 8°–14°N		Upper 200	1960s	56.9			Cushing (1971). Conversion from C m^{-2} to wet mass g m^{-2} from Hunt et al. (1981)
Canary Current 14°–21°N		Upper 200	1960s	40.2			Cushing (1971). Conversion from C m^{-2} to wet mass g m^{-2} from Hunt et al. (1981)
Canary Current 21°–28°N		Upper 200	1960s	80.4			Cushing (1971). Conversion from C m^{-2} to wet mass g m^{-2} from Hunt et al. (1981)
Canary Current 28°–33°N		Upper 200	1960s	43.3			Cushing (1971). Conversion from C m^{-2} to wet mass g m^{-2} from Hunt et al. (1981)
South Channel of Lawrence estuary Canada	Acoustics, 2 frequencies 38 and 120 kHz (Simrad Ek 60). Net sampling for sizes and species identification.		July 2002		85.6–235	Day	Cotte and Simard (2005). Scatter layers of *Euphausia superba* in the estuary. Area 25 km^2, survey time 3 days. Biomass estimated using target strength of individual weight
Elephant Island	Acoustics, one frequency 50, 120 or 150 kHz. Sizes from net samples		1981–1993 range mean		2.5–134.5 53.2		Hewitt and Demer (1994), *Euphausia superba*
South Georgia	Acoustics 2 frequencies 125 and 300 kHz		2002–2005 Winter 2002–2005 Summer		19.2 112.6		Saunders et al. (2007). From two moorings systems at 200 m. *Euphausia superba* biomass estimated using target strength.
Scotia Sea	Acoustics, 3 frequencies 38, 120 and 200 kHz (Simrad EK500)		January–February 2000		21.4		Hewitt et al. (2004). *Euphausia superba* biomass estimated using target strength.

[a] Macrozooplankon were not excluded but assumed of being highly underestimated by the net sampling.

estimations from traditional net sampling (Ayón et al., 2004) that is known to underestimate macrozooplankton biomass (Fleminger and Clutter, 1965; Debby et al., 2004), (ii) lies within the range of published macrozooplankton biomass in EBUS and other productive marine ecosystems and is lower than local biomass estimations from high abundance hot spots (Table 2), (iii) is comparable with other estimations performed in systems with high abundance of euphausiids (e.g., Cotte and Simard, 2005 for St. Laurent Estuary in Canada), (iv) is higher than macrozooplankton biomass from trophic models of the NHCS which have strongly underestimated the importance of macrozooplankton in the diet of anchovy and other main predators and have overestimated the macrozooplankton P/B ratio by at least 25% and (v) is coherent with both euphausiid life history parameters and predators' trophic ecology.

5. Conclusion

We performed the first high-resolution, large-scale acoustic macrozooplankton biomass estimation in an EBUS and provided a comprehensive view of the horizontal patterns of distribution of epipelagic macrozooplankton biomass according to the diel cycle. The total macrozooplankton biomass was estimated to about 105 g m^{-2} i.e., two to five times more than previous estimates. This new independent high biomass estimation of macrozooplankton is in agreement with the new finding in trophic ecology indicating that forage fish consume mainly macrozooplankton (Espinoza and Bertrand, 2008; Espinoza et al., 2009). Our results complement and support the current hypotheses proposed to explain the high fish production of the NHCS because (i) when compared with other EBUS, this system presents an intermediate upwelling intensity (Cury et al., 1998; Bakun and Weeks, 2008; Chavez and Messié, 2009), which favours zooplankton production (Ayón et al., 2008a), (ii) zooplankton production also benefits from the proximity of the NHCS to the equator as the high primary production combined with low wind-induced turbulence increases zooplankton feeding efficiency, (iii) the proximity of the NHCS to the equator also increases the residence time within this highly productive and less turbulent water (Bakun and Weeks, 2008) minimizing zooplankton loss due to advection and increasing zooplankton recruitment, (iv) El Niño events do not seem to have any strong detrimental effect on euphausiids (Brinton, 1967; Aronés et al., 2009), the main constituent of the zooplankton biomass, and finally, (v) according to anchovy feeding ecology a high biomass of euphausiids is needed to support the high biomass of anchovy.

The availability of continuous high-resolution (one data per second) information on macrozooplankton is a noticeable advantage compared with net sampling and provides a comprehensive vision of macrozooplankton distribution at a much lower cost than that of classic methods. However, net sampling (or alternative devices for zooplankton identification such as LOKI: Light-frame On-sight Key-species Investigation) will always be necessary to identify the observed organisms. The application of the method we developed opens a series of scientific perspectives. We are able to revisit present-day and historical acoustic databases and extract high-resolution data of macrozooplankton, a key ecological compartment of the ecosystem. Since zooplankton is the link between the physically driven primary producers and the biologically driven tertiary consumers, this information is essential to achieving a mechanistic understanding of the system, from physics to top predators. This high-resolution macrozooplankton information can be used to validate biogeochemical models, adjust trophic models and, more generally, to provide the "to" in end-to-end models (Mitra and Davis, 2010) of the NHCS. This would certainly further our understanding of how the NHCS functions on an ecosystem level. It allows, for instance, focusing research efforts on assessing the bottom-up physical effects of specific structures such as internal waves, filaments, ocean fronts or shallow epipelagic areas, on the patterns of distribution and abundance of a main compartment of the ecosystem. This study therefore represents a step toward the implementation of an ecosystem-based fisheries management.

Acknowledgments

This work is a contribution to the cooperation agreement between the Instituto del Mar del Peru (IMARPE) and the Institut de Recherche pour le Developpement (IRD) and of the LMI DISCOH. Michael Ballón was supported by an individual doctoral research grant (BSTD) proposed by the "Support and training of scientific communities of the South Department" (DSF) from IRD, managed by Egide. Myriax Software Pty. Ltd. kindly provided free access to Echoview.

References

Antezana, T., 2002. Adaptative behaviour of *Euphausia mucronata* in relation to the oxygen minimum layer of the Humboldt Current. In: Färber, Jaime. (Ed.), Oceanography of the Eastern Pacific II. Centro de Investigación Científica y de Educación Superior de Ensenada CICESE, México, pp. 29–40.

Antezana, T., 2010. *Euphausia mucronata*: a keystone herbivore and prey in the Humboldt Current system. Deep Sea Research Part II 57, 652–662. doi:10.1016/j.dsr2.2009.10.014.

Aronés, K., Ayón, P., Hirche, H.J., Schwamborn, R., 2009. Hydrographic structure and zooplankton abundance and diversity off Paita, northern Peru (1994 to 2004) – ENSO effects, trends and changes. Journal of Marine Systems 78, 582–598.

Ayón, P., Purca, S., Guevara-Carrasco, R., 2004. Zooplankton volume trends off Peru between 1964 and 2001. ICES Journal of Marine Science 61, 478–484.

Ayón, P., Criales-Hernandez, M.I., Schwamborn, R., Hirche, H.J., 2008a. Zooplankton research off Peru: a review. Progress in Oceanography 79, 238–255.

Ayón, P., Swartzman, G., Bertrand, A., Gutiérrez, M., Bertrand, S., 2008b. Zooplankton and forage fish species off Peru: large-scale bottom-up forcing and local-scale depletion. Progress in Oceanography 79, 208–214.

Bakun, A., 1996. Patterns in the Ocean: Ocean Processes and Marine Population Dynamics. University of California Sea Grant, San Diego, California, USA, in cooperation with Centro de Investigaciones Biológicas de Noroeste, La Paz, Baja California Sur, Mexico, 323pp.

Bakun, A., Weeks, S.J., 2008. The marine ecosystem off Peru: what are the secrets of its fishery productivity and what might its future hold? Progress in Oceanography 79, 290–299.

Barange, M., Pillar, S., 1992. Cross-shelf circulation, zonation and maintenance mechanisms of *Nyctiphanes capensis* and *Euphausia hanseni* (Euphausiacea) in the northern Benguela upwelling system. Continental Shelf Research 12, 1027–1042.

Barange, M., Stuart, V., 1991. Distribution patterns, abundance and population dynamics of the euphausiids *Nyctiphanes capensis* and *Euphausia hanseni* in the northern Benguela upwelling system. Marine Biology 109, 93–101.

Bertrand, A., Josse, E., Bach, P., Dagorn, L., 2003. Acoustics for ecosystem research: lessons and perspectives from a scientific programme focusing on tuna-environment relationships. Aquatic Living Resources 16, 197–203.

Bertrand, A., Gerlotto, F., Bertrand, S., Gutierrez, M., Alza, L., Diaz, E., Espinoza, P., Ledesma, J., Quesquén, R., Peraltilla, S., Chavez, F., 2008. Schooling behaviour and environmental forcing in relation to anchoveta distribution: an analysis across multiple spatial scales. Progress in Oceanography 79, 264–277.

Bertrand, A., Ballón, M., Chaigneau, A., 2010. Acoustic observation of living organisms reveals the upper limit of the oxygen minimum zone. PLoS ONE 5 (4), e10330. doi:10.1371/journal.pone.0010330.

Blackburn, M., 1979. Zooplankton in an upwelling area off northwest Africa: composition, distribution and ecology. Deep Sea Research Part I 24A, 41–56.

Brinton, E., 1962. The distribution of Pacific euphausiids. Bulletin of the Scripps Institution of Oceanography 8, 51–270.

Brinton, E., 1967. Vertical migration and avoidance capability of euphausiids in the California Current. Bulletin of the Scripps Institution of Oceanography 12, 451–483.

Brochier, T., Lett, C., Tam, J., Fréon, P., Colas, F., Ayón, P., 2008. An individual-based model study of anchovy early life history in the Northern Humboldt Current system. Progress in Oceanography 79, 313–325.

Chavez, F., Messié, M., 2009. A comparison of eastern boundary upwelling ecosystems. Progress in Oceanography 83, 80–96.

Chavez, F., Bertrand, A., Guevara-Carrasco, R., Soler, P., Csirke, J., 2008. The northern Humboldt Current system: brief history, present status and a view towards the future. Progress in Oceanography 79, 95–105.

Chu, D., Wiebe, P.H., 2005. Measurements of sound-speed and density contrasts of zooplankton in Antarctic waters. ICES Journal of Marine Science 62, 818–831.

Cotte, C., Simard, Y., 2005. Formation of dense krill patches under tidal forcing at whale feeding hot spots in the St. Lawrence Estuary. Marine Ecology Progress Series 288, 199–210.

Criales-Hernández, M., Schwamborn, R., Graco, M., Ayón, P., Hirche, H.J., Wolff, M., 2008. Zooplankton vertical distribution and migration off Central Peru in relation to the oxygen minimum layer. Helgoland Marine Research 62, 85–100.
Cury, P., Roy, C., Faure, V., 1998. Environmental constraints and pelagic fisheries in upwelling areas: the Peruvian puzzle. South African Journal of Marine Science 19, 159–167.
Cushing, D.H., 1971. Upwelling and the production of fish. Advances in Marine Biology 9, 255–300.
Debby, L., Jackson, G.A., Angel, M.V., Lampitt, R.S., Burd, A.B., 2004. Effect of net avoidance on estimates of diel vertical migration. Limnology and Oceanography 46, 2297–2303.
Escribano, R., Hidalgo, P., González, H., Giesecke, R., Riquelme-Bugueño, R., Manríquez, K., 2007. Seasonal and inter-annual variation of mesozooplankton in the coastal upwelling zone off central-southern Chile. Progress in Oceanography 75, 470–485.
Escribano, R., Hidalgo, P., Krautz, C., 2009. Zooplankton associated with the oxygen minimum zone system in the northern upwelling region of Chile during March 2000. Deep Sea Research Part II 56, 1083–1094.
Espinoza, P., Bertrand, A., 2008. Revisiting Peruvian anchovy (*Engraulis ringens*) trophodynamics provides a new vision of the Humboldt Current system. Progress in Oceanography 79, 215–227.
Espinoza, P., Bertrand, A., Van der Lingen, C.D., Garrido, S., Rojas de Mendiola, B., 2009. Diet of sardine (*Sardinops sagax*) in the northern Humboldt Current system and comparison with the diets of clupeoids in this and other eastern boundary upwelling systems. Progress in Oceanography 83, 242–250.
Fagetti, E., Campodonico, I., 1971. Larval development of the red crab *Pleuroncodes monodon* (Decapoda Anomura: Galatheidae) under laboratory conditions. Marine Biology 8, 70–81.
Fernandes, P.G., Korneliussen, R.J., Lebourges-Dhaussy, A., Masse, J., Iglesias, M., Diner, N., Ona, E., et al., 2006. The SIMFAMI Project: Species Identification Methods from Acoustic Multifrequency Information. Final Report to the EC, Q5RS-2001–02054.
Fleminger, A., Clutter, R.I., 1965. Avoidance of towed nets by zooplankton. Limnology and Oceanography 10, 96–104.
Foote, K.G., Knudsen, H.P., Vestnes, G., 1987. Calibration of Acoustic Instruments for Fish Density Estimation: A Practical Guide. ICES Cooperative Research Report 144.
Genin, A., 2004. Bio-physical coupling in the formation of zooplankton and fish aggregations over abrupt topographies. Journal of Marine Systems 50, 3–20.
Gerlotto, F., 1996.The gregariousness and behaviour of the pelagic fish: impacto of the acoustic evaluation and fisheries. In: Proceedings of Acoustic Seminar Akustican, vol. 2, May, 1996.
Greenlaw, C., 1979. Acoustical estimation of zooplankton populations. Limnology and Oceanography 24, 226–242.
Greenlaw, C., Johnson, R., 1982. Physical and acoustical properties of zooplankton. The Journal of the Acoustical Society of America 72, 1706–1710.
Guénette, S., Christensen, V., Pauly, D., 2008. Trophic modelling of the Peruvian upwelling ecosystem: towards reconciliation of multiple datasets. Progress in Oceanography 79, 326–335.
Gutiérrez, M., 2000. Estimados de biomasa hidroacústica de los cuatro principales recursos pelágicos en el mar peruano durante 1983–2000. Boletín Instituto del Mar del Perú 19, 139–156.
Gutiérrez, M., Ramirez, A., Bertrand, S., Móron, O., Bertrand, A., 2008. Ecological niches and areas of overlap of the squat lobster 'munida' (*Pleuroncodes monodon*) and anchoveta (*Engraulis ringens*) off Peru. Progress in Oceanography 79, 256–263.
Helly, J.J., Levin, L.A., 2004. Global distribution of naturally occurring marine hypoxia on continental margins. Deep Sea Research Part I 51, 1159–1168.
Hewitt, R.P., Demer, D.A., 1994. Acoustic estimated of krill biomass in the Elephant Island area: 1981–1993. CCAMLR Science 1, 1–5.
Hewitt, R., Watkins, J., Naganobu, M., Sushin, V., Brierley, A.S., Demer, D.A., Kasatkina, S., Takao, Y., Goss, C., Malyshko, A., Brandon, M., Kawaguchi, S., Siegel, V., Trathan, P., Emery, J., Everson, I., Miller, D., 2004. Biomass of Antarctic krill in the Scotia Sea in January/February 2000 and its use in revising an estimate of precautionary yield. Deep Sea Research Part II 51, 1215–1236.
Heymans, J.J., Baird, D., 2000. A carbon flow model and network analysis of the northern Benguela upwelling system, Namibia. Ecological Modelling 126, 9–32.
Hill, R.B., Johnson, J.A., 1974. A theory of upwelling over the shelf break. Journal of Physical Oceanography 4, 19–26.
Holliday, D.V., Pieper, R.E., 1995. Bioacoustical oceanography at high frequencies. ICES Journal of Marine Science 52, 279–296.
Horne, J.K., Jech, J.M., 1999. Multi-frequency estimates of fish abundance: constraints of rather high frequencies. ICES Journal of Marine Science 56, 184–199.
Hunt, G.L.J., Burgeson, B., Sanger, G.A., 1981. Feeding ecology of seabirds of the eastern Bering Sea. In: Hood, D.W., Calder, J.A. (Eds.), The Eastern Bering Sea Shelf: Oceanography and Resources, vol. 2. NOAA Univ. of Washington Press, Seattle, Washington, pp. 629–647.
Hutchings, L., Pillar, S., Verheye, H.M., 1991. Estimates of standing stock, production and consumption of meso- and macrozooplankton in the Benguela ecosystem. South African Journal of Marine Science 11, 499–512.
Jarre-Teichman, A., 1992. Steady-state Modelling of the Peruvian Upwelling Ecosystem. PhD Thesis, University of Bremen, Germany.
Johnson, R., 1977. Sound scattering from a fluid sphere revisited. Journal of the Acoustical Society of America 61, 375–377.
Kloser, R.J., Ryan, T., Sakov, P., Willliams, A., Koslow, J.A., 2002. Species identification in deep water using multiple acoustic frequencies. Canadian Journal of Fisheries and Aquatic Sciences 59, 1065–1077.
Konchina, Y.V., 1981. The Peruvian jack mackerel, *Trachurus symmetricus murphyi*, a facultative predator in the coastal upwelling ecosystem. Journal of Ichthyology 21, 46–59.
Konchina, Y.V., 1991. Trophic status of the Peruvian anchovy and sardine. Journal of Ichthyology 31, 59–72.
Korneliussen, R., 2000. Measurement and removal of echo integration noise. ICES Journal of Marine Science 57, 1204–1217.
Korneliussen, R.J., Ona, E., 2003. Synthetic echograms generated from the relative frequency response. ICES Journal of Marine Science 60, 636–640.
Kramer, D., Kalin, M.J., Stevens, E.G., Thrailkill, J.R., Zweifel, J.R., 1972. Collecting and Processing Data on Fish Eggs and Larvae in the California Current Region. NOAA Technical Report NMFS Circ-370, pp. 1–38.
Lavaniegos, B.E., Ohman, M.D., 2007. Coherence of long-term variations of zooplankton in two sectors of the California Current system. Progress in Oceanography 75, 42–69.
Lawson, G.L., Wiebe, P.H., Ashjian, C.J., Stanton, T.K., 2008. Euphausiid distribution along the Western Antarctic Peninsula. Part B: distribution of euphausiid aggregations and biomass, and associations with environmental features. Deep Sea Research Part II: Topical Studies in Oceanography 55, 432–454.
Lill, C.C., 1979. Upwelling over the Shelf Break. Journal of Physical Oceanography 9, 1044–1047.
Logerwell, E.A., Wilson, C., 2004. Species discrimination of fish using frequency-dependent acoustic backscatter. ICES Journal of Marine Science 61, 1004–1013.
Lu, B., Mackas, D.L., Moore, D.F., 2003. Cross-shore separation of adult and juvenile euphausiids in a shelf-break alongshore current. Progress in Oceanography 57, 381–404.
Mackas, D.L., Kieser, R., Saunders, M., Yelland, D.R., Brown, R.M., Moore, D.F., 1997. Aggregation of euphausiids and Pacific hake (*Merluccius productus*) along the outer continental shelf off Vancouver Island. Canadian Journal of Fisheries and Aquatic Sciences 54, 2080–2096.
MacLennan, D.N., Fernandes, P.G., Dalen, J., 2002. A consistent approach to definitions and symbols in fisheries acoustics. ICES Journal of Marine Science 59, 365–369.
Mathisen, O.L., 1989. Adaptation of the anchoveta (*Engraulis ringens*) to the Peruvian upwelling system. In: Pauly, D., Muck, P., Mendo, J., Tsukayama, I. (Eds.), The Peruvian Upwelling Ecosystem: Dynamic and Interactions, ICLARM, Conference Proceedings, vol. 18, pp. 220–234.
Mitra, A., Davis, C., 2010. Defining the "to" in end-to-end models. Progress in Oceanography 84, 39–42.
Mitson, R.B., Simard, Y., Goss, C., 1996. Use of a two-frequency algorithm to determine size and abundance of plankton in three widely spaced locations. ICES Journal of Marine Science 53, 209–215.
Mosteiro, A., Fernandes, P.G., Armstrong, F., Greenstreet, S.P.R., 2004. A Dual Frequency Algorithm for the Identification of Sandeel School Echotraces. ICES Document CM 2004/R: 12, 13pp.
Murase, H., Ichihara, M., Yasuma, H., Watanabe, H., Yonezaki, S., Nagashima, H., Kawahara, S., Miyashita, K., 2009. Acoustic characterization of biological backscatterings in the Kuroshio–Oyashio inter-frontal zone and subarctic waters of the western North Pacific in spring. Fisheries Oceanography 18, 386–401.
Napp, J.M., Ortner, P.B., Pieper, R.E., Holliday, D.V., 1993. Biovolume-size spectra of epipelagic zooplankton using a multi-frequency acoustic profiling system (MAPS). Deep Sea Research Part I: Oceanographic Research Papers 40, 445–459.
Neira, S., Arancibia, H., Cubillos, L., 2004. Comparative analysis of trophic structure of commercial fishery species off central Chile in 1992 and 1998. Ecological Modelling 172, 233–248.
Pakhomov, E.A., 2004. Salp/krill interactions in the eastern Atlantic sector of the Southern Ocean. Deep Sea Research Part II 51, 2645–2660.
Paulmier, A., Ruiz-Pino, D., 2009. Oxygen minimum zones (OMZs) in the modern ocean. Progress in Oceanography 80, 113–128.
Peterson, W., 1998. Life cycle strategies of copepods in coastal upwelling zones. Journal of Marine Systems 15, 313–326.
Postel, L., Fock, H., Hagen, W., 2000. Biomass and abundance. In: Harris, R., Wiebe, P., Lenz, J., Skjoldal, H.R., Huntley, M. (Eds.), Zooplankton Methodology Manual. Academic Press, San Diego, pp. 83–192.
Postel, L., da Silva, A.J., Mohrholz, V., Lass, H.U., 2007. Zooplankton biomass variability off Angola and Namibia investigated by a lowered ADCP and net sampling. Journal of Marine Systems 68, 143–166.
Ressler, P.H., Brodeur, R.D., Peterson, W.T., Pierce, S.D., Vance, P.M., Røstad, A., Barth, J.A., 2005. The spatial distribution of euphausiid aggregations in the Northern California Current during August 2000. Deep Sea Research Part II 52, 89–108.
Ryther, J.H., 1969. Photosynthesis and fish production in the sea. Science 166, 72–76.
Saunders, R.A., Brierley, A.S., Watkins, J.L., Reid, K., Murphy, E.J., Enderlein, P., Bone, D.G., 2007. Intra-annual variability in the density of Antarctic krill (*Euphausia superba*) at South Georgia, 2002–2005: within-year variation provides a new framework for interpreting previous 'annual' estimates of krill density. CCAMLR Science 1, 1–5.
Shannon, L., Moloney, C., Jarre, A., Field, J., 2003. Trophic flows in the southern Benguela during the 1980s and 1990s. Journal of Marine Systems 39, 83–116.
Simard, Y., Mackas, D.L., 1989. Mesoscale aggregations of euphausiid sound scattering layers on the continental shelf of Vancouver Island. Canadian Journal of Fisheries and Aquatic Sciences 46, 1238–1249.
Simmonds, J., MacLennan, D., 2005. Fisheries Acoustics. Theory and practices, second ed. Chapman & Hall, Berlin, 325pp.

Simmonds, J., Gutiérrez, M., Chipollini, A., Gerlotto, F., Woillez, M., Bertrand, A., 2009. Optimizing the design of acoustic surveys of Peruvian anchoveta. ICES Journal of Marine Science 66, 1341–1348.

Smith, J.N., Ressler, P.H., Warren, J.D., 2010. Material properties of euphausiids and other zooplankton from the Bering Sea. The Journal of the Acoustical Society of America 128, 2664–2680.

Stanton, T., Chu, D., 2000. Review and recommendations for the modelling of acoustic scattering by fluid-like elongated zooplankton: euphausiids and copepods. ICES Journal of Marine Science 57, 793–807.

Stanton, T., Chu, D., Wiebe, P.H., 1996. Acoustic scattering characteristics of several zooplankton groups. ICES Journal of Marine Science 53, 289–295.

Stanton, T.K., Wiebe, P.H., Chu, D., 1998. Differences between sound scattering by weakly scattering spheres and finite length cylinders with applications to sound scattering by zooplankton. Journal of the Acoustical Society of America 103, 253–254.

Swartzman, G., Hickey, B., Kosro, M., Wilson, C., 2005. Poleward and equatorward currents in the Pacific Eastern Boundary Current in summer 1995 and 1998 and their relationship to the distribution of euphausiids. Deep Sea Research II 52, 73–88.

Taki, K., 2006. Biomass and production of the euphausiid *Euphausia pacifica* along the coastal waters off north-eastern Japan. Fisheries Science 72, 221–232.

Tam, J., Taylor, M., Blaskovic, V., Espinoza, P., Ballón, M., Díaz, E., Wosnitza-Mendo, C., Argüelles, J., Purca, S., Ayón, P., Quipuzcoa, L., Gutiérrez, D., Goya, E., Ochoa, N., Wolff, M., 2008. Trophic modeling of the Northern Humboldt Current ecosystem. Part I: comparing trophic linkages under La Niña and El Niño conditions. Progress in Oceanography 79, 352–365.

Vinogradov, M.E., Shushkina, E.A., 1978. Some development patterns of plankton communities in the upwelling areas of the Pacific Ocean. Marine Biology 48, 357–366.

Walsh, J.J., 1981. A carbon budget for overfishing off Peru. Nature 290, 300–304.

Watkins, J.L., Brierley, A.S., 2002. Verification of the acoustic techniques used to identify Antarctic krill. ICES Journal of Marine Science 59, 1326–1336.

Wiebe, P.H., 1988. Functional regression equations for zooplankton displacement volume, wet weight, dry weight and carbon: a correction. Fishery Bulletin 86, 833–835.

Wiebe, P.H., Boyd, S.H., Cox, J.L., 1975. Relationships between zooplankton displacement volume, wet weight, dry weight, and carbon. Fishery Bulletin US 73, 777–786.

Zhu, Y., Tande, K., Zhou, M., 2009. Mesoscale physical processes and zooplankton transport–retention in the northern Norwegian shelf region. Deep Sea Research Part II 56, 1922–1933.